

The Calcium-Looping technology for CO₂ capture: On the important roles of energy integration and sorbent behavior

Antonio Perejón^{a,b}, Luis M. Romeo^c, Yolanda Lara^c,
Pilar Lisbona^c, Ana Martínez^c, Jose Manuel Valverde^{*d}

^aInstituto de Ciencia de Materiales de Sevilla (C.S.I.C.-Univ. Sevilla). C. Américo Vespucio 49, Sevilla 41092. Spain. ^bDept. de Química Inorgánica, Facultad de Química, Universidad de Sevilla, Sevilla 41071, Spain.

^cCIRCE (Research Centre for Energy Resources and Consumption), Universidad de Zaragoza, Mariano Esquillor 15, 50018 Zaragoza, Spain

^dFaculty of Physics, University of Seville, Avenida Reina Mercedes s/n, 41012 Sevilla, Spain

ABSTRACT:

The Calcium Looping (CaL) technology, based on the multicyclic carbonation/calcination of CaO in gas-solid fluidized bed reactors at high temperature, has emerged in the last years as a potentially low cost technology for CO₂ capture. In this manuscript a critical review is made on the important roles of energy integration and sorbent behavior in the process efficiency. Firstly, the strategies proposed to reduce the energy demand by internal integration are discussed as well as process modifications aimed at optimizing the overall efficiency by means of external integration. The most important benefit of the high temperature CaL cycles is the possibility of using high temperature streams that could reduce significantly the energy penalty associated to CO₂ capture. The application of the CaL technology in precombustion capture systems and energy integration, and the coupling of the CaL technology with other industrial processes are also described. In particular, the CaL technology has a significant potential to be a feasible CO₂ capture system for cement plants. A precise knowledge of the multicyclic CO₂ capture behavior of the sorbent at the CaL conditions to be expected in practice is of great relevance in order to predict a realistic efficiency from process simulations. The second part of this manuscript will be devoted to this issue. Particular emphasis is put on the behavior of natural limestone and dolomite, which would be the only practical choices for the technology to meet its main goal of reducing CO₂ capture costs. Under CaL calcination conditions for CO₂ capture (necessarily implying high CO₂ concentration in the calciner), dolomite seems to be a better alternative to limestone as CaO precursor. The proposed techniques of recarbonation and thermal/mechanical pretreatment to reactivate the sorbent and accelerate calcination will be the final subjects of this review.

*Corresponding author at: Faculty of Physics, Avda. Reina Mercedes s/n, 41012 Seville (Spain). Phone no. +34 954550960. Fax no. +34 954239434. Email: jmillan@us.es

41 1. Introduction

42

43 Carbon dioxide (CO₂) capture and storage, or CCS, is a process in which CO₂ is separated from
44 industrial and energy-related sources, compressed and transported to be stored underground or
45 used in other applications such as Enhanced Oil Recovery (EOR).¹⁻³ CCS is recognized as a
46 necessary technology for meeting greenhouse gas emissions reduction targets. Among the
47 different techniques under study, the Calcium Looping (CaL) technology is a potentially low
48 cost 2nd generation technology emerged in the last years.^{4,5} The process is based on the use of
49 CaO as a regenerable sorbent through carbonation/calcination cycles as schematized in Figure 1.
50 Thus, CO₂ present in the flue gas stream (in a volume concentration of ~15%) is captured by
51 partial carbonation of the CaO particles in a fluidized bed reactor (carbonator) operating at
52 650°C under atmospheric pressure. This temperature ensures a low value of the equilibrium CO₂
53 concentration (around 1% vol) and, at the same time, a fast enough reaction kinetics for
54 carbonation to take place in short residence times, which allows efficiently reducing the
55 concentration of CO₂ in the gas leaving the carbonator reactor.⁶ The partially carbonated
56 particles are subsequently circulated into a second reactor (calciner) where calcination of CaCO₃
57 to regenerate the sorbent is carried out at temperatures typically above 930°C under a highly
58 concentrated CO₂ environment of (between 70% and 90% vol). The CO₂ gas exiting the calciner
59 is thus ready for condensation, compression and transport. The high temperatures needed for
60 efficient calcination at practical rates is achieved by burning fuel in the calciner under a flow of
61 pure O₂ (oxycombustion) in order to avoid CO₂ dilution.⁷⁻⁹

62

63

64

65

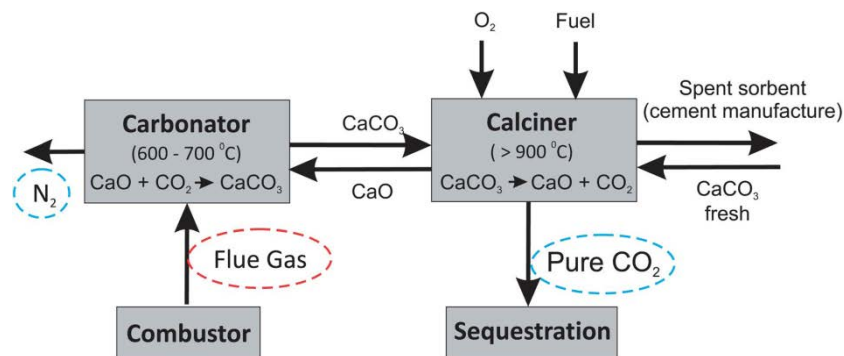
66

67

68

69

70



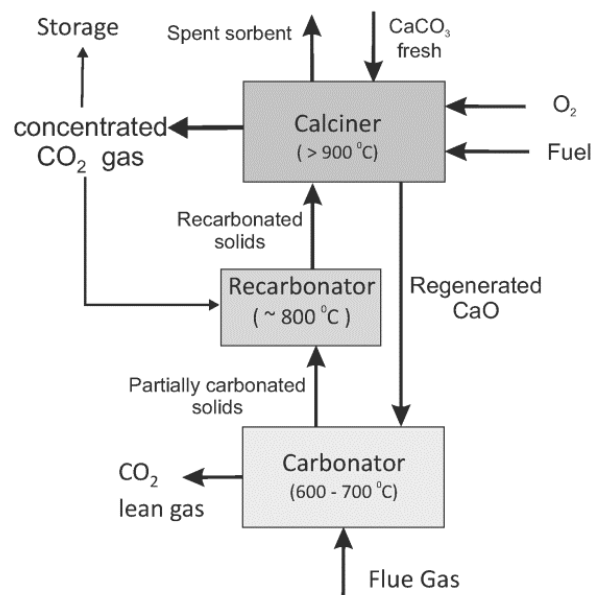
71

71 Figure 1. Schematic representation of the CaL process for CO₂ capture from post-combustion flue gas.
72 Reproduced with permission from reference [29]. Copyright 2013, Journal of Materials Chemistry A.

73

74 The CaL technology is being currently validated with success in pilot-scale coal fired plants of
75 1-2 MWth.⁸ The process is typically initiated by precalcining a batch of limestone (CaCO₃)
76 under air in the calciner, where the net production of CO₂ is only due to this initial calcination
77 step. Then, both the temperature and the CO₂ concentration in the calciner are increased by
78 starting operation in the oxycombustion mode. The produced CaO is taken to the carbonator

79 after which the carbonated solids obtained are circulated back to the calciner to regenerate CaO
 80 in the oxycombustion mode. One of the main issues of this process is CaO deactivation and the
 81 loss of fine sorbent particles generated by attrition that cannot be captured by cyclones.
 82 Therefore, it is necessary to periodically feed the calciner with a make-up flow of fresh
 83 limestone, which increases the demand of heat at the calciner.¹⁰⁻¹³ This inconvenience would be
 84 somewhat compensated by the low cost of natural limestone and the use of the purged CaO in
 85 other applications such as the cement industry or for desulphurization.¹⁴⁻¹⁶ However, it is
 86 recognized that the high consumption of fuel and oxygen in the calciner imposes an important
 87 energy penalty to the technology, and that enhancing the multicyclic activity of CaO would
 88 significantly improve the industrial competitiveness of the CaL technology.^{9, 17-20}
 89 A novel CaL concept aimed at minimizing the need of a large make up flow of fresh limestone
 90 is based on the recarbonation of the partially carbonated particles exiting the carbonator using
 91 the high CO₂ concentration gas stream available from the calciner (Figure 2). Multicyclic
 92 carbonation/recarbonation/calcination lab-scale tests suggest that the incorporation of a
 93 recarbonator would effectively enhance the capture efficiency and reduce the cost of the
 94 technology by reducing the required makeup flow of fresh limestone and thus the heat demand
 95 in the calciner.²¹⁻²⁵



111 Figure 2. Schematic representation of the Ca-looping process for post-combustion CO₂ capture modified
 112 by introducing an intermediate recarbonator reactor. Reproduced with permission from reference [25].
 113 Copyright 2014. Applied Energy.

115 In this manuscript we will review the main results published in the last 10 years on the effects of
 116 precalcination, carbonation and calcination conditions, as well as the effect of introducing a

117 recarbonation stage on the CO₂ capture performance of natural limestone and dolomite in the
118 CaL process. Even though there are many works published in the literature focused on the
119 synthesis of CaO based sorbents with enhanced carbonation activity,²⁶⁻²⁹ most of the sorbents
120 proposed are not compatible with the absolute necessity of reducing costs for the technology to
121 be developed at the commercial level. Thus, a part of this review will be focused on analyzing
122 the role of operating conditions on the multicyclic CO₂ capture capacity of the low cost natural
123 precursors of CaO, namely limestone and dolomite. As will be seen, lab-scale results suggest
124 that a modification on the operating conditions, within the constraints of the CaL process, could
125 bring about a significant improvement of the CO₂ capture capacity of CaO from these natural
126 precursors.

127

128 A further relevant aspect of the CaL technology that would contribute to improve the industrial
129 competitiveness of the process is the minimization of energy penalties. Different schemes of the
130 CaL process were originally proposed to match the need and supply of energy stream within the
131 loop.³⁰ Some of these possibilities have been later developed further, such as the use of a solid
132 heat carrier between the combustion chamber and the calciner in an indirect heat exchange; the
133 use of biomass in a joint combustor/carbonator reactor; or the use of pressurized fluidized beds.
134 The employ of solid carriers was developed by Lisbona et al.,³¹ and later by the combination of
135 CaL and chemical looping. The use of biomass in a joint combustor/carbonator reactor has been
136 developed in a 300kWth pilot plant in Spain,³² reaching 550h in combustion and in situ CO₂
137 capture mode. By integrating the CaL in biomass power plants, the fluidized bed combustor
138 may serve at the same time as carbonator operating at a temperature about 700°C to maximize
139 both biomass combustion and CO₂ capture. As regards the use of pressurized fluidized beds, it
140 has not received much interest. Just one work has explored the economic viability of this option,
141 which reports an efficiency of 40.7% and develops an economic model.³³ As conclusion, the
142 estimated cost per metric ton for CO₂ captured was \$23.7 (Canadian dollars), which is below the
143 cost of the amine scrubbing technology (39-96 \$/tCO₂ avoided).

144 The reduction of the energy demand in the CaL process has attracted the attention of many
145 researchers. In general, these works could be divided in two main options to minimize the
146 capture energy penalty. On one hand, we find some works aimed at reducing the energy
147 requirements of the capture cycle within the loop. On the other, there are studies whose main
148 goal is to recover the energy of the capture system by retrofitting the existing power plant or by
149 defining a new power plant that produces additional power.

150

151 The present review is organized as follows. Section 2 is devoted to review the methods
152 proposed to reduce the energy demand of the process by internal integration. In section 3 we
153 discuss the process modifications aimed at optimizing the overall efficiency by means of

154 external integration. The possibility of using the CaL technology in precombustion capture
155 systems and energy integration is described in section 4. The integration of CaL technology
156 with other industrial processes will be the subject of section 5. In the next sections we turn to
157 review results obtained on the CO₂ sorbent behavior at CaL conditions for post-combustion CO₂
158 capture with particular emphasis on natural limestone and dolomite. A review on the effects of
159 recarbonation and thermal/mechanical pretreatment for sorbent reactivation at CaL conditions
160 will be the final subjects of review.

161

162 **2. Reduction of the energy demand by internal integration**

163

164 The most recent proposals for internal heat integration in the CaL process to reduce energy
165 requirements follow two different strategies (i) to recover energy in the loop itself using a basic
166 CaL layout and (ii) to modify the traditional configuration of the cycle in order to avoid the
167 oxyfuel combustion step. Among the works focused on the first approach, Martínez et al.³⁴
168 analyzed different options to recover energy from the solids which leave the calciner prior to
169 enter the carbonator. The proposed layouts are oriented towards reducing the energy
170 requirements in the calciner which accounts up to a 37% of the total amount of heat in the
171 capture system.³⁵ Different configurations were studied to raise the temperature of the solid
172 sorbent stream fed to the calciner by internally integrating available heat flows. This reduction
173 in the calciner energy input may lead to a decrease in coal and oxygen consumptions which are
174 the cause of the main energy penalties. The use of a mixing seal valve to transfer heat between
175 particles is one of the most interesting proposals. In this device, solids exchange heat directly,
176 although this mixture leads to a reduction of the fraction of active CaO in the particle population
177 flowing from the seal valve to the carbonator. Also, the inclusion in the CaL system of an
178 additional circulating fluidized bed, acting as a heat recovery device, was proposed to exchange
179 heat from the gas leaving the calciner to the solids leaving the carbonator.

180 A further modification of the process would consist of the inclusion of a cyclonic preheater
181 (Figure 3a) to transfer energy from the gas leaving the calciner to the solids that reacted in the
182 carbonator.¹⁸ Several cyclonic heat exchangers consisting of different number of steps were
183 modelled. The results obtained from the simulation of a CaL system with a two-step cyclonic
184 preheater showed a power of 127 MW transferred to the solids. This internal heat exchange
185 led to a 13.3% of reduction in the mass ratio of coal consumed to CO₂ captured as compared
186 to the ordinary configuration (0.39 kgcoal/kgCO₂ vs 0.45 kgcoal/kgCO₂). Furthermore, oxygen
187 needs for oxyfuel combustion were reduced in a similar proportion (11%). The energy
188 efficiency of the cycle, quantified as the ratio of the heat flow available for integration in a
189 steam cycle to the thermal heat supplied by the coal in the calciner, was also assessed and the
190 study showed that there was no significant energy penalty associated.

191 The CaL system including a mixing seal valve was thoroughly analyzed by Martínez et al.³⁶ In
192 this configuration, the solids can directly exchange heat albeit the mixing of the particles
193 reduces the fraction of active CaO entering the carbonator. Either a fraction of the flue gas from
194 the power plant or a fraction of the CO₂ stream exiting the calciner might be used to fluidize the
195 seal valve (Figure 3b). These options were assessed by Martínez et al.³⁶, and the independent
196 use in the returning channels of both gas streams was finally proposed. The mass ratio of
197 consumed coal to captured CO₂ was 0.38 kgcoal/kgCO₂ (15.5%), and the oxygen consumption
198 decreased by a 14.5% similarly to the reductions obtained with the cyclonic preheater.

199 With the same target of reducing the process irreversibilities and limiting energy penalty of the
200 process, Kim et al.³⁷ propose a process with multiple stages which operates at different
201 temperature levels. In each stage the sorbent is recirculated between an absorber and a
202 regenerator (Figure 3c). The concept is analogous to that presented elsewhere for amine
203 scrubbing.³⁸ In this case there is an intra-stage heat integration from the high temperature
204 carbonator to medium temperature regenerator. Thus, the high temperature energy availability
205 for an additional steam cycle is reduced, which would decrease the size and the capital cost of
206 the new power plant. This configuration has been suggested for other sorbents such as K₂CO₃,
207 Na₂CO₃ promoted MgO and Li₄SiO₄ for the low (30-200°C), medium (300-500°C) and high
208 temperature (550-750°C) stages.³⁷ Heat integration is proposed directly between hot and cold
209 sorbent particles of different stages, and indirectly using heat transfer media for the intra-stage
210 integration. For a capture efficiency of 85% and natural gas as a fuel in the high temperature
211 regenerator, researchers reported a net electrical efficiency in a power plant associated with this
212 high temperature looping of 34.9% for an adjusted three-stage process. That means an
213 efficiency penalty of 9.5% in the power plant. There is an important room for improvement in
214 this scheme as integration has not been completely defined, and operating conditions were not
215 optimized.

216 One of the main penalties associated to the CaL cycle is the need of an air separation unit to
217 obtain pure O₂ for calcination by oxy-fuel combustion. Different modified CaL schemes have
218 been proposed lately to overcome this disadvantage. The process called “HotPSA” works with
219 pressure swing absorption.³⁹⁻⁴¹ The main target is to drive both the carbonation/calcination
220 reactions near equilibrium by maintaining the temperature in a small range and modifying the
221 pressure to affect the CO₂ partial pressure. The temperature range in both reactors is between
222 650 and 900°C for carbonation and calcination reaction rates to be high enough. The calciner
223 needs steam injection (Figure 3d) or depressurization to reduce the CO₂ partial pressure. The
224 advantages of this process would include a long life for the sorbent by the reduction of loss of
225 fast carbonation reactivity due to sintering as well as the elimination of oxy-fuel combustion
226 (avoiding additional coal, oxygen and ASU consumption, and oxy-fuel CO₂ compression). This

227 leads to some options for recovering the waste heat not used in the calcination and the flue gas
 228 energy in a new steam cycle to compensate energy penalties.

229

230

231

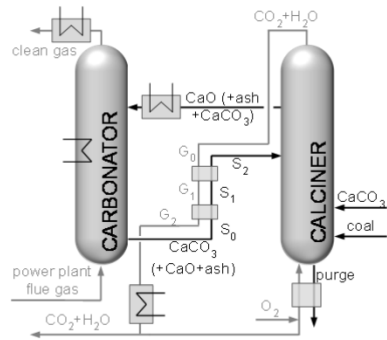
232

233

234

235

236

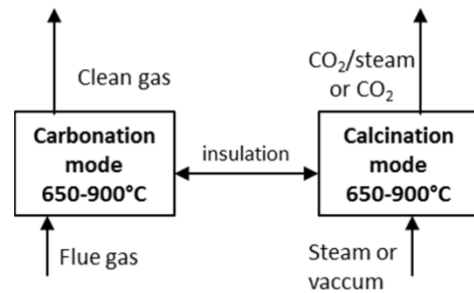


237 a) Cyclonic preheater scheme (adapted from reference [18])

237

238

239



239 d) HotPSA process (adapted from reference [39])

240

241

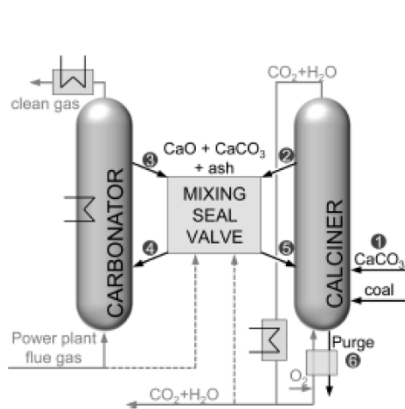
242

243

244

245

246

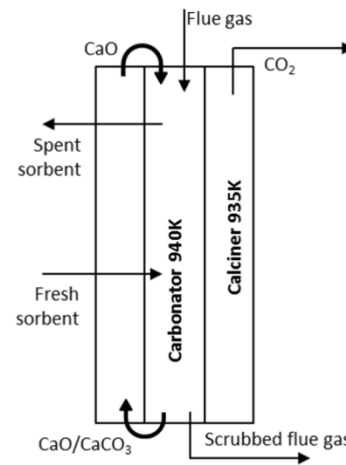


246 b) Mixing seal valve scheme (reproduced from reference [36])

247

248

249



249 e) Endex Ca-Looping process (adapted from reference [40])

250

251

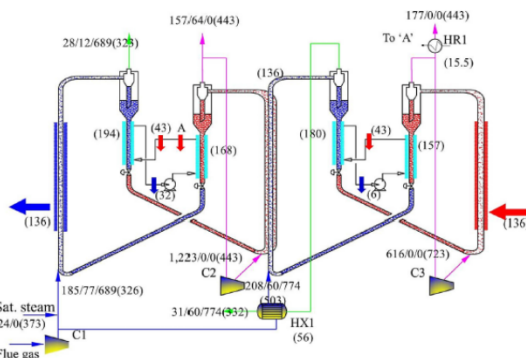
252

253

254

255

256



256 c) Two-stages process scheme (reproduced from reference [37])

258

259

260

261

262

263

Figure 3. Configurations for internal energy integration. Reproduced with permission from references [18], [36], [37], [39] and [40].

Direct heat transfer exchange between combustor/calciner or calciner/carbonator has been developed in the Endex configuration.⁴² This process involves direct thermal coupling of the

264 carbonator and the calciner. In this configuration it is assumed that the endothermic process in
265 the calciner will occur at a higher temperature than that of the carbonator, which can be
266 achieved by maintaining the calciner pressure lower than that of the carbonator. In the Endex
267 system, the endothermic reaction is driven directly by the heat released by the exothermic one.
268 The rate of heat transfer has an exponential component due to the temperature dependence of
269 the endothermic reaction rate. This configuration proposes a completely different system layout
270 (Figure 3e) in which the carbonator is housed inside the calciner, and the entire unit is thermally
271 insulated without the need for additional heat in the system. Due to the system characteristics,
272 an important control parameter is the sorbent mass flow rate. The pressures and temperatures of
273 the reactors are considerably lower than in the ordinary CaL, being just 0.048 bar for the
274 carbonator and 0.002 bar for the calciner.⁴⁰ This process cannot be compared in energy terms
275 with the conventional CaL. Exergy-based analysis has been performed in order to compare both
276 processes,⁴⁰ and also to assess the entropy generation of the sub-processes of the Endex
277 configuration.⁴³ The energy requirements of operation at very low pressures and the increase of
278 power demand in CO₂ compression may hinder the potential advantages of this configuration.
279 Another possible scheme consists of a sequential capture of SO₂ and CO₂ using
280 deactivated/spent CaO for flue gas sulphation at 900°C before being injected to the carbonator.¹⁴
281 This option implies a complete modification of the power plant. Flue gas at high temperature
282 has to be introduced to the sulphation reactor at 900°C, thus it is not possible to recover heat
283 from flue gases before this reactor. Energy has to be recovered between sulphation and
284 carbonation (650°C) reactors and from the clean gas after the carbonation. Moreover, the energy
285 released in the exothermic reaction within the carbonator and from the CO₂ exiting the calciner
286 at high temperature (~930°C - 950°C) have to be recovered.

287

288 **3. Optimizing the overall efficiency by external integration**

289

290 The traditional approach for external heat integration was proposed by Romeo et al.⁴⁴ They
291 designed a highly integrated system in which the energy released by the CaL process was
292 integrated in a supercritical steam cycle. From then, a supercritical steam cycle with single
293 reheat has been the preferred system to integrate the recovered heat from the CaL. The state of
294 the art of these power plants includes steam conditions of 250 bar and 540-560 °C and net
295 efficiency of 44%.⁴⁵ Such parameters could increase the overall system efficiency and reduce
296 the specific CO₂ emissions (kgCO₂/kWh_e).

297 Energy sources in the CaL process come mainly from three high-temperature flows: the
298 exothermic heat from the carbonation reaction (Q_{carb}), the flue gas stream leaving the carbonator
299 ($Q_{\text{flue gas}}$) and the CO₂ stream leaving the calciner ($Q_{\text{CO}_2 \text{ out}}$); and two low-temperature streams:
300 the CO₂ stream through the compression ($Q_{\text{CO}_2 \text{ comp}}$) and the purge flow (Q_{purge}). Also, heat from

301 the coolers in the ASU compression step (Q_{ASU}) and heat from the particles circulating from the
 302 calciner to the carbonator ($Q_{solids\ CL\ to\ CR}$) have the potential to be used. The works analyzed take
 303 advantage of these streams to define the bottoming steam cycle, although not all of them make
 304 use of the whole set of streams listed. Table 1 summarizes the energy sources used in each
 305 work.

306

307

308 Table 1. Energy sources

309

Reference	High temperature sources				Low temperature sources		
	Q_{carb}	$Q_{flue\ gas}$	$Q_{CO2\ out}$	$Q_{solids\ CL\ to\ CR}$	Q_{purge}	$Q_{CO2\ compression}$	Q_{ASU}
Romeo 2008 [44]	X	X	X		X		
Romeo 2009 [20]	X	X	X	X	X	X	
Hawthorne 2009 [46]	X	X	X			X	
Romano 2009 [47]	X	X	X			X	
Yang 2010 [48]	X	X	X				
Lisbona 2010 [49]	X	X	X	X	X	X	
Martínez 2011 [50]	X	X	X		X	X	
Vorrias 2013 [51]	X	X	X		X	X	X
Lara 2013 [52]	X	X	X	X	X	X	
Lara 2014 [53]	X	X	X	X	X	X	

320

321

322 In Romeo et al.,⁴⁴ an initial supercritical steam cycle was first defined and then modified to take
 323 advantage of the energy flows of the CaL cycle, with the aim of avoiding the need for an extra
 324 boiler. The supercritical cycle was divided into five zones (Reheat, In-boiler, Economizer, High-
 325 and Low-pressure feedwater heaters) depending on their temperature levels. This system
 326 reduced the reference plant CO_2 emission from 0.781 $kgCO_2/net-kWh$ to a value of 0.122
 327 $kgCO_2/net-kWh$, and obtained a net efficiency of 37.04 %; which translates to an energy penalty
 328 of 7,89 efficiency points (see Table 1).

329 To complement this option, an exergy analysis was presented to assess the conventional CaL
 330 process with a different integration point of view.⁵⁴ It took advantage of the vast amount of high
 331 quality energy to retrofit the power plant or to develop a new steam cycle. Romeo et al. used the
 332 pinch and the exergy analysis to define an optimum window for the integration of a CaL process
 333 and their retrofit in a coal power plant.⁵⁴ The waste heat from the CO_2 capture was used to
 334 produce steam in the original power plant. The exergy recovered as high pressure steam should
 335 be around 70% of the total exergy; while the exergy for reheating the steam amounts 25%. The
 336 low temperature heat released in the intercoolers pertaining to CO_2 compression may be used to
 337 reduce the steam bleed to low pressure regenerative heaters.

338 Several researches calculated the effect of the CaL process when applied to power stations on
 339 their efficiency. An overview of the integration results obtained in different works is
 340 summarized in Table 2. The drop in efficiency reported is between 6 and 8 efficiency points.^{30,}
 341 ⁵⁵ Other works have reported energy penalties of 7.5 eff-points for a capture efficiency in the
 342 carbonator of 70% or 10.4% eff-points for a capture efficiency in the carbonator of 90%.⁵⁰
 343 Hawthorne et al. modeled the CaL process and its integration taking into account also the
 344 available heat of the CO₂ compression unit.⁴⁶ In this case, the reference power plant is a 1052
 345 MW_e coal-fired plant, and the energy penalty after integration is 6.4 percentage points. Due to
 346 the high temperature (high exergy) of the CaL cycles, the optimization of the integration with a
 347 power plant is an essential subject that has to be studied in detail.

348
 349

350 Table 2. Net power and net efficiencies comparison

351

Reference	Reference plant		Capture plant		Reference + capture + integrated plant			
	Net power (MW)	Efficiency (%)	CO ₂ capture efficiency (%)	Amount of heat recovered (MW)	Net power (MW)	Efficiency (%)	Energy penalty	CO ₂ avoided cost (€/ton)
Romeo 2008 [44]	427,5	44,93	85,00	--	619,80	37,04	7,89	15,77
Romeo 2009 [20]	500*	40,32	--	--	--	--	--	13,20
Hawthorne 2009 [46]	1052,0	45,60	80,00	1624,0	1533,00	39,20	6,40	--
Romano 2009 [47]	630,8	44,18	97,04	--	452,40	37,35	6,83	--
Yang 2010 ^v [48]	600,0	40,60	85,00	906,6	846,00	36,80	3,80	28,90
Lisbona 2010 [49]	500,0	38,11	--	--	709,50	32,33	5,78	15,80 [¥]
Martínez 2011 [50]	350,0	36,00	70,00-90,00	--	--	--	8,30-10,30 ^x	--
Vorrias 2013 [†] [51]	304,15	39,05	94,00	524,0	428,2	34,09	4,96	--
Lara 2013 [52]	474,0	38,23	85,00	838,9	714,50	32,04	6,19	--
Lara 2014 [53]	474,0	38,23	85,00	841,9	738,10	33,06	5,17	--

362 * Gross power
 363 ^v Only case 4 shown
 364 [¥] For generic natural limestone, 6€/ton CO₂ and low attrition
 365 [†] Only case A shown
 366 ^x Range w/o including a cement plant

367
 368
 369 Some works have analyzed possible integrations of the CaL process in a reference power plant.
 370 Yang Yongping et al.⁴⁸ studied for a 600 MW_e one-reheat power plant the integration of five
 371 cases depending on the use of the recovered heat: i) to replace extracted steam from the
 372 turbines; ii) to replace part of the boiler heat load; iii) to replace the extracted steam from the
 373 turbines and part of the boiler heat load; iv) to build a heat recovery steam generator and
 374 produce steam to drive new turbines; v) to replace the extracted steam in the new steam cycle.

375 The option of using the heat in a HRSG and drive new turbines was selected as the best
376 efficiency option (penalty of 3.8 efficiency points), the largest power output (net 846 MW_e) and
377 the lower cost of CO₂ avoided (28.9 €/tCO₂). This analysis also showed that although case iv
378 was not the one with largest total heat recovery, the efficiencies do not follow the same trend.
379 These efficiencies depend both on the amount of heat and the type of thermal energy use. The
380 option that replaces part of the boiler heat load showed the worst results in net power, efficiency
381 and costs. The rest of the options need a detailed analysis since replacing bleeding from the
382 steam turbine requires additional developments.

383 A similar scheme was proposed by Vorrias in 2013.⁵¹ They used as a reference a 330 MW_e
384 lignite power plant with a supercritical single reheat boiler. In this scheme, concentric L-valves
385 were used as solid recirculation heat exchangers. As in previous papers, a secondary steam cycle
386 with single reheat is used to take advantage of the energy released by the CaL process. In the
387 high temperature section, the design included a split of the steam production in the carbonator
388 and calciner sections. The last one included the single reheater. In the low temperature section,
389 part of the energy from CO₂ compression and ASU coolers is integrated in the steam cycle as
390 low pressure heaters. There is no detailed information about the temperature profiles but a final
391 potential heat for district heating is described. This agrees with the fact that in this CCS option
392 there is huge amount of low temperature waste energy available. The energy content of the
393 purge is used to increase the oxygen and recirculated CO₂ temperatures. One of the important
394 novelties of this work is the analysis of the influence of lignite pre-drying on fuel consumption
395 and capture efficiency showing no effect on the carbonator capture efficiency.⁵¹ Fuel pre-drying
396 decreased the fuel demands in the calciner and the CaL system was smaller (less additional
397 power production) and more efficient. Both are important advantages as this scheme would
398 require less capital and operational costs. In case that there is no heat exchange between solids,
399 the effect on the overall efficiency was small but the system was considerably bigger. An
400 evaluation of the CaL technology as a retrofit option showed higher overall net electrical
401 efficiency when compared to chemical absorption with MEA or oxy-fuel combustion power
402 plants. The energy penalty of the CaL process was below 5 efficiency points (Table 2) versus
403 the 7.8 of MEA or 5.85 of oxy-fuel combustion. The only disadvantage of this CaL scheme is
404 that the size of the overall system is higher than the other post-combustion processes, 82% than
405 MEA and 53% than oxy-fuel. For a new built power plant with CCS based on the CaL process
406 the overall efficiency increased up to 34.04% including the capture process.

407 The carbonation conversion of the sorbent and the heat requirements at the calciner are key
408 variables that influence the performance of CaL systems. Several studies have been devoted to
409 analyze the influence of the capture cycle parameters in the global system, considering not only
410 the capture step but their energy integration, to determine the CO₂ avoided costs. Romeo et al.
411 recommended avoiding operating conditions with low-recirculation rates and purge percentages

412 over 5% to optimize the cost per tonne of CO₂ avoided.²⁰ In this work, the minimum CO₂
413 avoided cost, Table 2, is obtained for a molar CaO/CO₂ ratio of 5 and a purge of 1.5%. In this
414 analysis, heat recovery steam generators take advantage of the flue gas from carbonator at
415 650°C and from calciner at 930°C. A solid-gas heat exchanger is used to reduce the purge
416 temperature down to 180°C. Intercooling CO₂ compression heat is used in low-pressure heat
417 exchangers in the condensate section of the steam cycle.

418 The effect of the decay of carbonation conversion with increasing number of
419 carbonation/calcination cycles was addressed in Romeo et al.¹² and Lisbona et al.⁴⁹, which
420 maintain the same heat integration scheme. Romeo et al.¹² studied the competitiveness of CaO
421 based synthetic sorbents with enhanced sorption behavior as compared to natural limestone.
422 Simulations calculated the maximum price for enhanced sorbents to achieve a reduction in CO₂
423 removal cost under different process conditions (solid circulation and make-up flow). The
424 results obtained in this study may be used as an assessment tool of new sorbents to understand
425 what prices would be competitive as compared to natural limestone in the CaL capture systems.
426 After analyzing the requirements of limestone and enhanced sorbents, on the basis of their
427 multicyclic sorption capacity and the pair purge-CaO/CO₂ ratio, the possible use of sorbents
428 other than natural limestone was assessed. In Lisbona et al.,⁴⁹ doped limestone, dolomite and
429 synthetic sorbents were simulated within the system. In most cases, the increased cost of sorbent
430 synthesis and/or limestone modification leads to a significant increase of the cost of the system
431 operation and therefore CO₂ capture cost. Any comparison among sorbents will be accurate only
432 if both chemical and economic considerations are taken into account in the study. Lisbona et al.
433 present a common basis for sorbent comparison, including the influence of attrition processes in
434 the model.⁴⁹ The integration of the sorbent cost and its chemical and mechanical performance
435 were studied for different options. The aim was to compare the CO₂ avoided cost as a function
436 of average conversion of solid population and cost for different sorbents. Despite improved
437 conversion results, the unit cost of the sorbent is crucial to maintain the CaL concept
438 economically attractive. Moreover, it must be remarked that most of lab-scale studies reported
439 in the literature on the multicyclic CO₂ capture behavior of synthetic sorbents are carried out
440 under not realistic CaL conditions. As will be seen in the second part of this review, the
441 behavior of a sorbent may change dramatically when CaL operating conditions are changed.

442 The work of Martínez et al. determined the operating conditions in a CaL cycle that minimize
443 the energy penalty when implemented in an existing power plant with 36% net efficiency.⁵⁰ To
444 evaluate energy penalties associated with the capture system, a reference plant consisting on the
445 existing subcritical one and a new hypothetical supercritical power plant with the same fuel
446 input as the calciner was assumed. Different integration possibilities were studied depending on
447 the operating conditions in the CaL cycle. The highest thermal efficiencies were obtained for the
448 cases with lowest make-up flow; in which the modest activity of the sorbent is compensated by

449 high-solids flow between reactors to maintain the desired carbonation efficiency, which agrees
450 with the results obtained by Romeo et al.²⁰

451 Wang et al. simulated in Aspen Plus an integration of the CaL cycle using Ca(OH)₂ as sorbent
452 with different cases: one ideal case which is not very realistic, an industrial case and one acid
453 case to determine the effect of Ca(OH)₂ on the removal of all acid gases present in flue gas.⁵⁶
454 For the ideal case, a minimum energy penalty (additional thermal energy input into the system)
455 of 5.8% is showed for an indirect-fired calciner and a minimum CO₂ compression energy of 75
456 kWh/tonne. One additional efficiency gain could be achieved by modifying the ASU
457 consumption from 200 to 167 kWh/tonne O₂. The industrial case included non-ideal heat
458 transfer and increases the CO₂ compression and ASU consumption. In this case the energy
459 penalty ranged from 13 to near 16% for a 100% heat extraction efficiency and indirect-fired
460 calciner. Considering the use of coal in the calciner, the penalty ranged from 16 to more than
461 24% depending on the coal.

462 Usually, researchers have focused on coal-fired power plants for application the of CaL process.
463 Flue gas CO₂ concentrations range between 10-17 vol%; much higher than in NG power plants
464 where typical CO₂ volume concentration in flue gas is around 3-5%. In spite the lower CO₂
465 partial pressure of NG combined cycle, the outlet temperature of the gas turbines around 600°C
466 makes interesting the analysis of the possibilities of integration of the CaL cycle into NGCC
467 power plants.^{57,58} Moreover, the lower CO₂ partial pressure reduces the carbonator temperature
468 down to 600°C. The CaL cycle could be located directly after the GT before any Heat Recovery
469 Steam Generator without incurring in exergy losses due to temperature changes. The scheme for
470 the integration of the energy streams in a bottoming cycle will be different to the usual HRSG in
471 NGCC or the previous coal-fired power plants.⁵⁷ Berstad et al. (32) reported several simulations
472 with/without heat integration within the CaL and using a standard/advanced/super-critical steam
473 cycle as bottoming cycle to take advantage of the energy streams in the CCS.⁵⁷ Assuming a
474 reference NGCC efficiency of 58.1%, the application of MEA chemical absorption reduces in
475 8.6 points the efficiency. In spite of the use of advance/super-critical steam cycle the design
476 with CaL cycle reduced the efficiency between 10.0-11.5 eff-points. Again, it was shown that
477 the use of internal heat integration reduces the size of the overall installation, in this case around
478 12%. Authors concluded that the CaL process is not competitive for NGCC in comparison with
479 MEA chemical absorption. Nevertheless, in a later work with synthetic sorbents the authors
480 claimed an efficiency loss of only 5.0 points for super-critical turbine (7.1 and 6.8 for natural
481 limestone and synthetic CaO/MgO).⁵⁸ The main variables affecting the power plant efficiency
482 were the internal heat recuperation and the CO₂ recycle temperature. To increase the process
483 flexibility the configuration included two HRSG and a primary and a secondary steam cycle and
484 a reduction of the calciner temperature to 900°C.

485 Manovic and Anthony demonstrated experimentally the feasibility of a new approach to
486 eliminate the oxyfuel combustor: the combination of CaL with a chemical looping using CuO as
487 oxygen carrier. In their work, they developed, prepared and tested a composite material
488 consisting of CaO as CO₂ acceptor and CuO as oxygen carrier.⁵⁹ In the same work, three
489 alternative routes were proposed to implement the concept. Further techno-economic analysis
490 should determine the better integration option. Another experimental study carried out by Ridha
491 et al. compares the use of in-house developed composite CaO-CuO material with the use of a
492 mixed bed of CaO and CuO pellets.⁶⁰ The results showed a better performance of the mixture of
493 pure materials despite of the inherent advantages of composite materials.

494 We can conclude that the most important advantage of the high temperature CaL process is the
495 use of the high temperature streams that could reduce significantly the energy penalty associated
496 with CCS. As reported previously, there are several works in the literature that show and
497 quantify important penalty reductions. Nevertheless, it is essential to optimize the results
498 through a well established method. The pinch methodology, combined with economic and
499 exergetic analysis to optimize the design of the heat exchangers network is addressed in Lara et
500 al. where four configurations integrating the same amount of heat than the base case were
501 studied.⁵² The design and analysis of these configurations to determine the optimum for the
502 system, according to energy, exergy and economic criteria were undertaken, and the cycle
503 efficiency was improved by the relocation of the heat exchangers. The results obtained in this
504 work are further distilled in the algorithm shown in Lara et al.,⁵³ aiming to provide a systematic
505 procedure for heat integration of this type of systems to find an energy and cost-efficient
506 solution for the heat exchanger network, to simplify the integration process. In this work, a
507 procedure based on pinch analysis was proposed and tested in two different cases. In both
508 scenarios the integration was designed to take advantage of all the available heat from the
509 process to power the bottoming supercritical steam cycle, thus quantifying the minimum energy
510 penalty (5.17 eff-points, Table 2). A sensitivity analysis for each process was also performed,
511 and the heat exchangers network obtained through the algorithm was the most economical one.
512 Finally, a future modelling challenge is the dynamic simulation of the CaL process. Recently,
513 some attempts have been done but it will be necessary to the flexibility of the capture systems in
514 a power plant load following scenario.⁶¹

515

516 **4. Energy integration of CaL in precombustion capture systems**

517

518 The CaL cycle provides a number of benefits when coupled with fuel gasification or reforming
519 as precombustion capture process. The heat released in the carbonation reaction is used to run
520 the endothermic in-situ steam reforming or the gasification reactions, leading to an overall
521 autothermic reaction. Another benefit derived from the presence of CaO is the shifting of the

522 equilibrium to greater hydrogen yields. The subsequent calcination of the CaCO_3 to regenerate
523 the sorbent is however a significant problem still to be solved for precombustion CO_2 capture
524 systems. The high temperature heat demanded in the calcination stage and the heat transfer
525 mechanism is in practice quite problematic. Different configurations have been adopted to
526 integrate the CaL process in a precombustion process for enhanced hydrogen production and
527 minimize the energy penalty associated to sorbent regeneration. The basic configuration
528 includes the application of oxycombustion of a solid fuel in the calciner itself to provide the
529 energy required. Several studies have been focused in the integration of this CaL basic
530 configuration with steam reforming of gaseous fuels (sorption enhanced reforming, CaL-SER)
531 and solid fuel gasification.^{62, 63}

532

533 **4.1 Sorption enhanced reforming (SER) – CaL integration**

534

535 Although the industrial process used to produce hydrogen, namely steam methane reforming, is
536 a mature commercial technology, there are still a number of issues for further improvement. In
537 particular, diverse reactor concepts, which combine several process stages within a single unit,
538 are being investigated. Significant enhancement of the process is achieved by addition of a CO_2
539 sorbent to the reactor, which shifts the reversible reforming and water gas shift (WGS) reaction
540 beyond their thermodynamic limitation.⁶⁴

541 The complexity of CaL-SER processes relies in the fact that a single reactor is used to carry out
542 hydrocarbon catalyzed reforming, carbonation and water-gas shift reaction. Potential energy
543 savings associated to the autothermal overall reaction was initially estimated by Ortiz and
544 Harrison in a 20%.⁶⁵ Experimental tests have proved the process in both small fixed-bed and
545 fluidized bed reactors. Depending on reaction conditions of temperature, pressure and steam to
546 carbon ratio, the content of hydrogen in the final gas is in the range 95-99%.^{62, 63}

547 More recently, Connell et al. assessed from a techno-economic point of view the integration of
548 CaL with a steam methane reforming plant.⁶⁶ Their results showed a 9% reduction of cost in the
549 production of hydrogen (production rate of hydrogen 25579 kg/h) mainly related to the benefits
550 obtained from the generation of electricity (189 MWe of net electric power) in a steam cycle
551 driven by the waste heat released in CaL.

552

553 **4.2. CaL enhanced gasification**

554

555 The production of hydrogen from solid fuel gasification may be coupled to the CaL process for
556 increasing the hydrogen content in the syngas. Under this scenario, WGS reaction with in situ
557 CO_2 removal, sulphur and halide removal are integrated in a single reactor in the absence of
558 WGS catalyst. The reactor is fed with the syngas from the gasifier after being cooled down.

559 Ramkumar and Fan conducted thermodynamic analysis which showed the positive effect of Ca-
560 based sorbents in the WGS reaction and in the purity of the obtained hydrogen (over 99%).⁶⁷
561 They conducted also a number of experimental tests, which showed a worse behavior of the
562 sorbent for higher temperatures but a correct operation of the concept at near-stoichiometric
563 steam to carbon ratios without WGS catalysts. The waste heat from the CaL process would be
564 used to generate steam and co-produce electricity in a steam turbine. In the techno-economic
565 study presented by Connell et al.,⁶⁶ the extra produced net electricity power with respect to a
566 same-size coal-to-hydrogen plant without CaL CO₂ capture is estimated to be 319 MWe. The
567 same study points out that the reduction of the cost of hydrogen or electricity relative to the base
568 plant is found to be 12%.

569 Apart from these conventional gasification followed by syngas upgrading stage, a more
570 ambitious configuration was HyPr-RING (hydrogen production by reaction-integrated novel
571 gasification).⁶³ HyPr-RING was developed in Japan and the challenge was to carry out the in-
572 situ CO₂ capture in a coal gasifier reactor fed with coal, steam, and Ca-based sorbent. The CO₂
573 content in the produced syngas should directly react with CaO, thus enhancing the amount of H₂
574 produced via the WGS reaction. In the regenerator, the oxyfuel combustion of non-reacted coal
575 provided enough energy to regenerate the sorbent. An intermediate stage of hydration was
576 included to prevent sorbent degradation. The gasifier/carbonator operated at 600-700°C and 3
577 MPa, which resulted in slightly over 50% carbon conversion and around 90% H₂ in the syngas
578 corresponding to a cold gas efficiency above 77%. The regenerator was operated at 800°C and
579 0.1 MPa. Similar proposals for in-situ gasification with CaL CO₂ removal have also been
580 analyzed by Florin and Harris using biomass and low grade fuels.⁶⁸ This second concept (in-situ
581 gasification and CO₂ capture with CaO) has been demonstrated by Abanades et al. in the pilot
582 plants of INCAR.⁶⁹

583

584 **4.3. Integrated gasification combined cycle (IGCC) – CaL integration**

585

586 Several researchers have investigated the utilization of syngas from gasification and CaL
587 upgrading process in electricity production. An advanced concept of power plants includes a
588 CaL gasifier/regeneration integrated with a combined Brayton/Rankine cycles, IGCC-CaL.

589 Connell et al. technically compared through simulations an IGCC CaL plant and a reference
590 case of IGCC plant with commercial CO₂ capture.⁶⁶ Both systems had the same gasifiers and
591 combustion turbines. The carbonator in the IGCC CaL operates at greater pressure compared to
592 hydrogen production gasification, because the pressure inlet to the turbine is greater to the
593 pressure specifications for high purity hydrogen. This results in a higher temperature
594 requirement in this reactor (700°C). The syngas generated in this process does not require H₂O
595 removal since it serves as a diluent of the fuel to achieve the required heating value. A metallic

596 filter is required before the turbine inlet to retain possible solid particles. The calciner was
597 exclusively fired by coal. Their results showed a reduction of costs of 12% in comparison with
598 the base case. The proposed system processed 374 ton/h of coal, which generated a net power of
599 932.9 MW with CO₂ capture efficiency above 99% and a net efficiency near 33% HHV.

600 The exergy efficiency of the integrated concept was analyzed through detailed simulation by
601 Siefert et al.⁷⁰ In the Brayton cycle, the air ratio was fixed in order to have a temperature of
602 1600K and a pressure of 1.62 MPa. In the Rankine cycle, superheated steam was introduced to
603 high pressure turbine at 625°C and 20 MPa and reheated to the same temperature at 2MPa. The
604 condenser operated at 0.02 MPa and a temperature spring form 136°C to 50°C. The proposed
605 system gasifies 29 ton/h of coal and generates 112 MW of electric power (67MW Brayton
606 cycle, 48 Rankine cycle, 3 MW fuel expander) which corresponds to an exergetic efficiency of
607 46.4%. The capture efficiency of the system is 66.6% and the normalized CO₂ emission rate is
608 0.23 kg CO₂/kWh.

609 An economic assessment of IGCC CaL coupled systems has been done by Cormos by analyzing
610 the integration of CaL and a coal gasification plant, which consists of an oxygen-blown
611 gasifier.⁷¹ The power plant generates around 545-560 MW of net power presenting a net
612 efficiency of 37% and a capture efficiency above 90%. The inclusion of the CaL technology
613 increases between 24-42% the specific capital investment while O&M and LCOE costs are
614 increased in the ranges 24-30% and 39-48%, respectively. Specific CO₂ emissions were
615 estimated to be around 0.30-0.35 kg CO₂/kWh.⁷²

616

617 **4.4. Integrated Gasification Fuel Cell (IGFC) – CaL integration**

618

619 Another advanced solid fuel based power plant coupled with CaL CO₂ capture is the integration
620 of enhanced gasification and fuel cells. The removal of CO₂ prior entering the fuel cell reduces
621 the content of CO and CO₂ and avoids carbon deposition while keeping a significant amount of
622 methane in the gaseous fuel. This methane can be internally reformed in the solid oxide fuel cell
623 (SOFC), which reduces cooling costs and parasitic loads. H₂S is also removed from the syngas
624 without the need of being condensed and re-injected before entering the anode side of the
625 SOFC. CO₂ and H₂S may be removed by lime inside or just after the gasifier which significantly
626 reduce the size and consumptions of the equipment.

627 One of the first proposals in this direction was the ZEC process developed by Los Alamos
628 National Laboratory.⁶³ Coal is hydrogasified to produce methane. Once the solid fuel is
629 converted to methane, the gaseous fuel is subjected to a CaL-SER process as described above.
630 Half of the produced hydrogen is used in the hydrogasification step and the remaining will
631 produce electricity in a solid oxide fuel cell. The high temperature off-gas from the fuel cell is
632 used to regenerate the spent sorbent. A system analysis estimated coal to electricity conversion

633 efficiency of 68.9% including CO₂ capture and compression. Although the project is no longer
634 pursued by ZECA, research on these topics has continued in the Cambridge University and
635 Imperial College. Dean et al. (40) gather those investigations done at laboratory scale on
636 different critical aspects.⁶³

637 Based on promising experimental results on the field of CaL enhanced steam gasification of
638 coal, Xu et al. investigated the performance of the entire process consisting of two fluidized bed
639 reactors, a gasifier/carbonator and a regenerator.⁷³ Thermodynamic simulations of a similar
640 concept of SOFC fed with upgraded syngas were performed using Aspen Plus.⁷³ The obtained
641 syngas presented an amount of hydrogen above 95%. Considering the system heat balance, the
642 optimal operation conditions were 650°C and 3MPa in the gasifier and 900°C and 0.1 MPa in
643 the oxyfuel regenerator with a steam to carbon ratio of 3. The cold gas efficiency was 92.6%.
644 The integration of a SOFC- gas turbine (SOFC-GT) hybrid cycle with the enhanced gasification
645 process accounts for an equivalent power efficiency of CO₂ capture and compression of 61.9%.
646 Siefert et al. analyzed a system that integrates a CaL enhance gasifier with a solid oxide fuel cell
647 from an exergetic and economic point of view.⁷⁰ The SOFC operating parameters which
648 maximized the internal rate of return on investment were a pressure of 300 kPa, a current
649 density of 1.0 Acm⁻², an air stoichiometric ratio of 2.0 and a fuel utilization of 80%. The system
650 gasifies 29 ton/h of coal and has an AC power output of 143 MW (116 MW is generated by the
651 SOFC, 23 MW by the combined air compressor and exhaust expander and 9 MW by the fuel
652 expander). Near 70% of CO₂ is captured and sent to compression which corresponds to a
653 normalized CO₂ emission rate of 0.16 kg CO₂/kWh. The exergy efficiency was found to be
654 between 40-65% depending on the value of the SOFC operating variables which is much higher
655 than traditional IGCC-CCS concepts.

656

657 **4.5. Unmixed fuel processing**

658

659 Some approaches have tried to overcome the issue of high energy consumption in the
660 regeneration stage of the CaL process from substituting oxyfuel combustion in the calciner
661 reactor by an unmixed chemical combustion process.⁷⁴ The unmixed fuel process consists of
662 three coupled reactors: a gasifier/reformer, a sorbent regenerator and a reactor to oxidize an O₂
663 transfer material, which produces a high temperature/high pressure vitiated air. This technology
664 has the potential to eliminate the need for the air separation unit.

665 The concept was integrated and analyzed by Lisbona and Romeo,³¹ which considered the
666 utilization of syngas obtained through CaL enhanced gasification of coal in a SOFC to produce
667 electricity, the inclusion of two gas turbines to take advantage of the energy contained in the
668 flue gases from afterburner and calciner and a steam cycle with steam produced from heat
669 recovery. The oxygen carrier used in the regeneration stage was FeO. The influence of steam to

670 carbon ratio in gasifier and regeneration reactor, pressure of the system, temperature for oxygen
671 transfer material oxidation, purge percentage in calciner, average sorbent activity and oxidant
672 utilization in fuel cell were analyzed. An electrical efficiency up to 73% was reached under
673 optimal conditions and CO₂ capture efficiencies near 96% ensure a good performance for
674 climate change mitigation targets.

675 The application of this concept to in-situ enhanced biomass gasification has been more recently
676 investigated by Rahman et al.⁷⁵ Instead of using a mixture of pellets, they have developed
677 composite CaO/CuO materials and demonstrated experimentally the technical feasibility of the
678 integration. Three sequences were simulated through testing. Two of them implied the use of
679 composite materials and the third one used a mixture of separated CaO and CuO pellets. Results
680 showed some difficulties related to reduction capacity loss in combining both materials in one
681 pellet. Given the promising integration of both technologies using a dual loop, further research
682 must be pursued especially through the testing of both types of pellets together.

683 Abanades et al. proposed the inclusion of a second chemical loop in which a reversible redox
684 reaction between copper and oxygen takes place.⁷⁶ The technical solution consisted of three
685 interconnected reactors; i) a sorption enhanced reformer where hydrogen is produced by
686 catalyzed steam reforming of natural gas and CO₂ is captured simultaneously, ii) a regenerator
687 of CaCO₃ using the heat released from the reduction of CuO with a gas fuel and iii) the
688 oxidation of Cu to CuO with air. The high efficiency of heat transfer between calcination and
689 copper reduction reactions allows moderating temperatures and saving energy. The proposed
690 scheme is reported as one single reactor operating in batch mode switching between three
691 operation modes: A) in which the fixed bed initially contains CaO and Cu to allow sorption
692 enhanced reforming reaction (slightly exothermic); B) when the oxidation of Cu with nitrogen-
693 rich air (under specific temperature and pressure to avoid CO₂ release) takes place; and C)
694 performing CaCO₃ regeneration and reduction of CuO to Cu. In this last mode the reactor
695 maintains a temperature between 800-900°C under atmospheric pressure or lower. Gases
696 obtained in the B mode are sent to a gas turbine, whose electric efficiency is maximized by
697 burning part of the hydrogen produced in the A mode to increase mass flow and temperature.
698 Overall CO₂ capture efficiency is over 80% when 87% of H₂ is burnt in the gas turbine. Energy
699 efficiency to hydrogen is 58% (H₂/CH₄). There is no complete heat integration so the overall
700 energy efficiency of the process is not calculated but it is expected to be high since energy
701 penalty processes have been avoided. The presence of solids in the calciner has to be optimized
702 depending on the fed fuel to minimize the demand for additional heat. The calculations must be
703 validated through experimental and modelling work.

704

705

706

707 **5. Integration of the CaL technology with other industrial processes**

708

709 The CaL technology may be also integrated with other industrial processes leading not only to a
710 reduction of the CO₂ emissions but also to an improvement of the operation of those processes.
711 This is the case of the concentrated solar power (CSP) generation and the paper and cement
712 industries.

713 There are two ways in which CSP may be integrated with the CaL cycle. On one hand, CSP
714 may be used to provide energy to the calciner for the regeneration reaction in order to reduce the
715 fuel consumption associated with the CO₂ capture process (Figure 4a). On the other hand, the
716 CaL cycle may be used as a thermal storage system to storage the unstable solar energy
717 production for future use, thus avoiding the disadvantage derived from the production
718 variability (Figure 4b). In regards to the former, Zhang et al. examined the energy efficiency of
719 the CaL system when the calciner is driven by a combination of oxyfuel combustion and CSP.⁷⁷
720 In this system, a fraction of the CO₂ leaving the calciner is used as a heat transfer fluid in the
721 solar collectors and then it is recycled to the regeneration reactor. Therefore, a reduction of the
722 fossil fuel consumption in the calciner is obtained, entailing a decrease of the additional CO₂
723 generated and a diminution of the mass flow rate of fresh limestone.

724

725

726

727

728

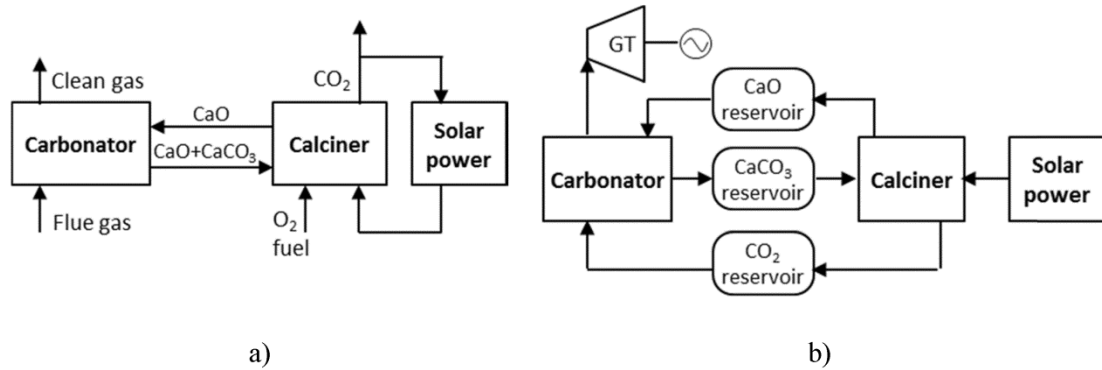
729

730

731

732

733



734 Figure 4. Calcium looping integration with concentrated solar power.

735

736

737 As mentioned, the CaL process may be used as a thermochemical storage system integrated
738 with the concentrated solar power generation. It has the advantages of operating at high
739 temperatures and having significant energy density compared to most sensible and latent storage
740 technologies. However, besides the development of a solar calciner, there are some challenges
741 to be faced since high carbonation activities and high pressure in the carbonator are required.
742 Edwards et al. determined that the optimal sorbent activity should be in the range 20% – 40%

743 and the carbonator should operate at 800 – 900 °C at 2.8 – 9.1 bar to achieve plant efficiencies
744 between 40% - 46%.⁷⁸

745 Regarding the paper industry, Sun et al. analyzed the possibility of using lime mud,⁷⁹ which is a
746 solid waste resulting from the causticization reaction in alkali recycling process, as sorbent in
747 the CaL cycle. Results showed a stable carbonation conversion of 21% from 2 to 100 cycles.
748 Better results were obtained when a pre-wash was carried out to reduce the chlorine content,
749 thus avoiding its negative effect on sintering and carbonation conversion. In this case, a 36%
750 carbonation conversion was obtained after 100 cycles. Also the effect of hydration of the CaO
751 derived from both the lime mud and the pretreated lime mud was analyzed obtaining a further
752 enhancement of the capture capacity, especially in the first cycles.

753 The integration of the cement industry and the CaL technology has been broadly studied since
754 the production of cement is one of the industrial sectors with the biggest carbon footprint and
755 makes use also of limestone as a raw material for the clinker manufacture. Moreover, the CaL
756 retrofitting capacity makes this integration a promising combination not only for future designs
757 but also for existing cement plants. Different degrees of integration may be achieved depending
758 on the aspects coming into play: i) Most proposed schemes focus on the integration of mass
759 flows (Figure 5a); the CO₂ generated in the cement plant is captured in the CaL cycle and the
760 purged sorbent is directed to the cement plant to feed the precalciner or the rotary kiln.⁸⁰⁻⁸² ii) In
761 other studies, the heat flows are also involved (Figure 5b). Romeo et al. proposed an integration
762 scheme in which a fraction of the waste heat from the CaL cycle was used to preheat the air
763 entering the cement plant.⁸³ The whole system comprises a power plant and a cement plant,
764 from which the CO₂ is captured, the CaL process, and a steam cycle to make use of the surplus
765 energy from the capture system and the cement plant. Results showed that this synergy may
766 permit 94% of CO₂ avoided emissions with an interesting cost, 12.4 €/tCO₂. iii) Lastly, even the
767 sharing of a reactor has been proposed.^{84, 85} Rodríguez et al. presented a scheme in which the
768 CaL calciner and the cement plant precalciner are the same reactor and the flue gas from the
769 rotary kiln is directed to the carbonator (Figure 5c).⁸⁴ They compared this system with the use of
770 an oxy-fired precalciner obtaining higher CO₂ capture efficiency, 99% and 89% respectively,
771 and avoided CO₂ cost, 23 \$/tCO₂ and 16 \$/tCO₂ respectively. Romano et al. proposed a
772 configuration with an oxyfuel calciner, shared by CaL and cement plant, and a carbonator
773 integrated in the raw meal suspension preheater process (Figure 5d).⁸⁵ Results showed a CO₂
774 capture efficiency of 95.4% with this scheme.

775

776

777

778

779

780

781

782

783

784

785

786

787

788

789

790

791

792

793

794

795

796

797

798

799

800

801

802

803

804

805

806

807

808

809

810

811

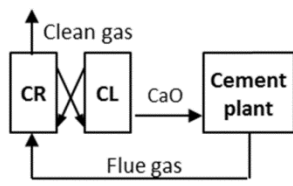
812

813

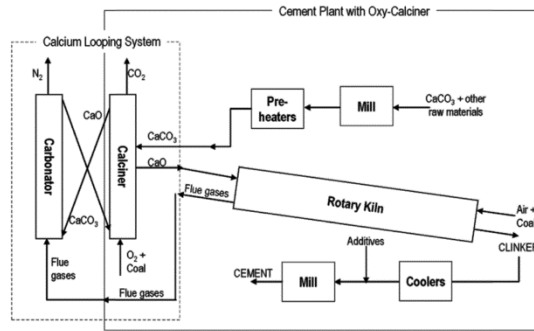
814

815

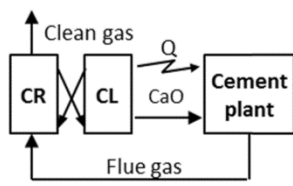
816



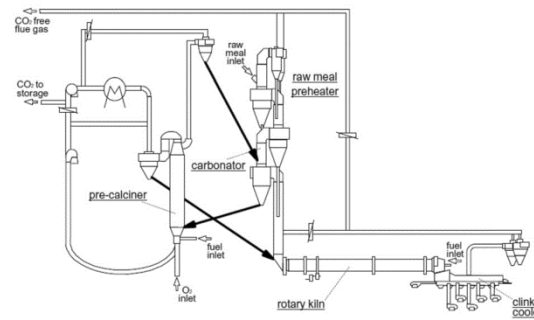
a)



c) reproduced from reference [84]



b)



d) reproduced from reference [85]

Figure 5. Calcium looping integration with cement plants. Reproduced with permission from references [84], [85].

Using the purged sorbent from the CaL calciner to feed a cement plant has the advantage of reducing the CO₂ generated in the cement manufacture. The CO₂ from the calcination and that generated in the combustion required to provide the energy for this reaction is avoided. Moreover, the raw material costs and the energy consumption of the ensemble cement plant and CaL process are reduced. However, the demands imposed on cement composition may limit this potential synergy. Dean et al. analyzed the limiting factors taking part.⁶³ Purged material consists mainly of CaO, a less significant fraction of ashes, calcium sulphate and trace elements released from fuel. Regarding the later, the maximum sulphur content of the ordinary portland cement is about 2.5% - 3% to avoid the expansion and cracking of the cement paste upon hydration and a reduction of the strength properties. Repeated exposure of trace elements contained in the fuel to the calciner environment over a long series of cycles may cause undesired effects on cement properties. Furthermore, attrition and agglomeration may affect the cement production since fines may be entrained and coarser particles may reduce the material burnability. Atsonios et al. analyzed the effect of different fuels on purge sulphur content concluding that the use of petcoke leads to an undesirable proportion of this compound.⁸⁰ They

817 proposed an intermediate gasification step as a petcoke pretreatment method to reduce the
818 sulphur presence in the purge.

819 The use of other CO₂ capture technologies, mainly amine scrubbing and oxy-fuel combustion,
820 in combination with cement manufacture has also been analyzed and compared with the use of
821 the CaL technology.^{80, 82, 84-86} The CaL energy consumption per kg of captured CO₂ has been
822 calculated to be 0.43 – 0.68 times higher than that of the oxy-fuel combustion and 0.61 - 1.89
823 times lower than that of the amine scrubbing.⁸⁶ The CaL process has the highest energy
824 recovery potential, 3.8 times higher than that of the oxy-fuel combustion and 11.5 times higher
825 than that of the amine scrubbing.⁸² Regarding CO₂ capture efficiency, the best results are
826 obtained with the CaL technology, 90% - 100%, against a 63% - 89% in the case of the oxy-fuel
827 combustion and around 85% for the amine scrubbing.^{80, 82, 84-86} As a conclusion, the CaL
828 technology has a significant potential to be a feasible CO₂ capture system for cement plants.

829

830 **6. Lab-scale test results on the multicyclic CaO capture capacity at CaL conditions**

831

832 A precise knowledge of the multicyclic carbonation reactivity of the Ca-based sorbent is of
833 paramount importance to assess the CO₂ capture efficiency and cost of the CaL technology. The
834 reaction kinetics and CO₂ capture capacity of Ca-based sorbents are usually evaluated by means
835 of thermogravimetric analysis (TGA) lab-scale tests. Realistic CaL conditions to be expected in
836 practice involve: i) short residence times (on the order of a few minutes), ii) low CO₂
837 concentration (about 15% in volume) for carbonation at temperatures around 650°C, iii) high
838 temperature and high CO₂ concentration in the calciner for sorbent regeneration and
839 precalcination of the makeup flow of solids (temperatures above 930°C and CO₂ vol% of at least
840 70% in volume, respectively) and iv) very fast transitions between the carbonation and
841 calcination stages (of just a few seconds).^{13, 87} The fluidized bed carbonator and calciner reactors
842 would be operated in the fast fluidization regime, which ensures an optimum transfer of heat
843 and mass. TGA tests provide optimum mass and heat transfer by using limestone samples of
844 very small mass (just about 10 mg) at contact with the gas. However, the common furnaces
845 usually employed in TGA tests to assess the multicyclic sorbent behavior are characterized by
846 low heating rates (of about 10°C/min) between the carbonation and calcination stages that are
847 not representative of the real process.⁸⁸ The use of TG analyzers based on infrared heating by
848 halogen lamps allows varying the temperature at a very fast and controlled rate (300°C/min for
849 heating and cooling), thus shortening the transitions between the carbonation and calcination
850 stages to just tens of seconds, which adjusts better to conditions to be expected in the real
851 application.^{89, 90}

852 A common observation from TGA tests is that carbonation takes place in two well differentiated
853 phases (Figure 6). In a first fast carbonation stage, CO₂ is chemisorbed on the available free

854 surface of the CaO particles until a thin layer of CaCO₃ (40-50 nm thick) is formed.
 855 Carbonation continues in a second relatively slower stage characterized by diffusion through the
 856 solid CaCO₃ layer.

857

858

859

860

861

862

863

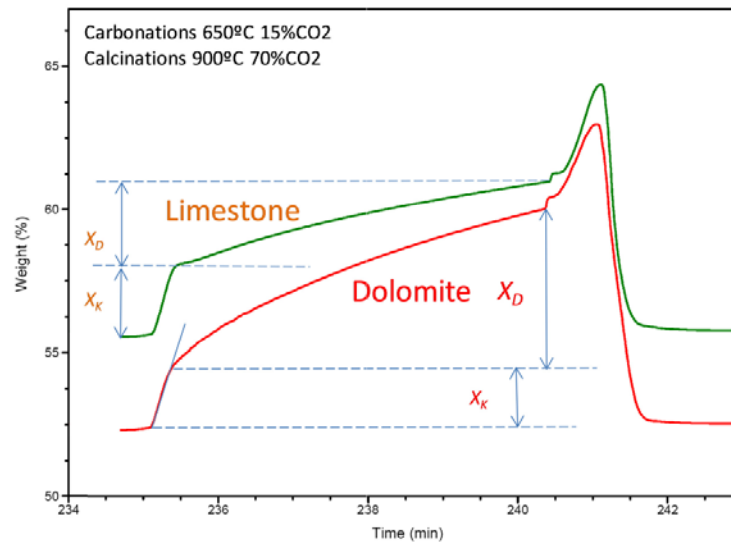
864

865

866

867

868



869

870

871

872

873

874

875

876

877

878

879

880

881

882

883

884

885

886

887

888

889

890

891

892

Figure 6. Time evolution of sorbent weight % during a carbonation/calcination cycle for limestone and dolomite measured by TGA⁹¹ showing in the detail the existence of a fast carbonation phase and a relatively slower phase during carbonation (carbonation for 5 min at 650°C under 15% CO₂; calcination for 5 min at 900°C under 70% CO₂. Cycle number 20). The overshoot at the end of the carbonation stage is due to a short recarbonation under high CO₂ partial pressure at the transition to calcination stage that takes place while the temperature has not reached yet the equilibrium temperature.

It is usually believed that most of carbonation taking place in residence times of a few minutes occurs in the fast carbonation stage, which is driven by the reaction kinetics.⁹² However, TGA tests carried out under calcination environments of high CO₂ partial pressure show otherwise.^{91, 93-95} As may be seen in Figure 6, carbonation in the solid-state controlled diffusion phase (X_D as compared to X_K in the fast phase) represents a significant contribution to the overall carbonation. The substantial relevance of diffusion controlled carbonation when calcination is carried out at realistic conditions of high CO₂ partial pressure remains yet to be taken into account in the formulation of carbonator models to scale-up the technology.⁷

Ideally, the sorbents should react fast toward an optimum capture capacity and maintain it independently of the number of calcination/carbonation cycles. However, the multicyclic conversion of CaO decays progressively with the cycle number, mainly due to the decrease of available surface area as a consequence of material sintering during calcination at high temperature.^{4, 17, 96, 97} CaO conversion is defined as the ratio of mass of CaO converted in each carbonation stage to the mass of CaO initially present in the sorbent after calcination. TGA tests show that the CaO multicyclic conversion in short residence times can be described by the following expression:⁹⁸

$$\frac{X_N}{X_1} = \frac{X_r}{X_1} + \left[\frac{1}{k(N-1) + (1 - X_r/X_1)^{-1}} \right]; (N = 1, 2 \dots) \quad (1)$$

893

894 where N is the cycle number, X_1 is CaO conversion in the first cycle, k is the deactivation
 895 constant and X_r is the residual conversion, which is asymptotically approached after a large
 896 number of cycles.

897

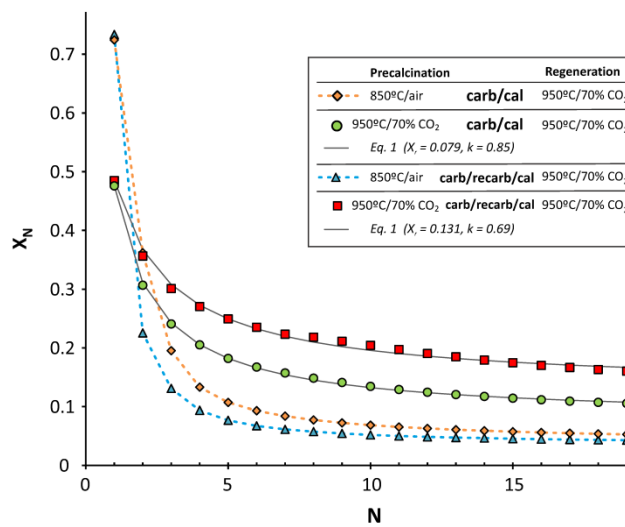
898 **7. The multicyclic CO₂ capture capacity of natural limestone at CaL conditions**

899

900 Limestone stands as the most suitable CaO precursor to guarantee the industrial competitiveness
 901 of the CaL technology.^{12, 15} However, the porous skeleton obtained from calcination of
 902 limestone suffers severe sintering usually attributed to lattice diffusion at the high temperatures
 903 of calcination, which causes a progressive reduction of the CaO surface area with the cycle
 904 number, and therefore an irreversible loss of CaO conversion.^{99, 100} TGA tests involving
 905 calcination at 950°C under low CO₂ concentration show that multicyclic CaO conversion decays
 906 with the cycle number and converges to a residual value $X_r = 0.07-0.08$.^{21, 92, 101, 102} The presence
 907 of CO₂ at high concentration in the calcination environment produces a significantly marked
 908 drop of conversion for CaO derived from limestone precalcined in air, with values around 0.05
 909 after few cycles.^{33, 89, 90, 103} It has been proposed that a progressive growth of the regenerated
 910 crystal structure along preferential surfaces, which are more stable but less favorable for CaCO₃
 911 nucleation, could play a role on the loss of multicyclic CaO conversion.¹⁰⁴⁻¹⁰⁶ On the other hand,
 912 empirical results seem to indicate that decarbonation in CO₂ is a complex process involving a
 913 two-stage reaction mechanism, which consists of the endothermic chemical decomposition of
 914 CaCO₃ to yield CO₂ and adsorbed CO₂, followed by CO₂ desorption and exothermic structural
 915 transformation of CaO from a metastable CaO* form to the stable phase.¹⁰⁷ Thus, at low CO₂
 916 partial pressures, desorption of CO₂ is fast, but at high CO₂ partial pressures and high
 917 temperatures hindered desorption of CO₂ and the exothermicity of CaO structural
 918 transformation would hamper calcination.¹⁰⁸

919 Figure 7 compares multicyclic CaO conversion data obtained for limestone samples precalcined
 920 at 850°C (heated at 20°C min⁻¹) in air and at 950°C (heated at 300°C min⁻¹) under 70% CO₂ and
 921 30% air vol/vol. The former conditions would replicate precalcination of the initial batch of
 922 limestone in the practical application, while the latter mimic precalcination of the fresh makeup
 923 of limestone introduced in the calciner to compensate for sorbent losses and deactivation.
 924 Subsequent carbonation/calcination (carb/cal) cycles consisted of 5 minutes of carbonation at
 925 650°C under 85% air and 15% CO₂ (vol/vol), and 5 minutes of calcination at 950°C under 70%
 926 CO₂ and 30% air (vol/vol).

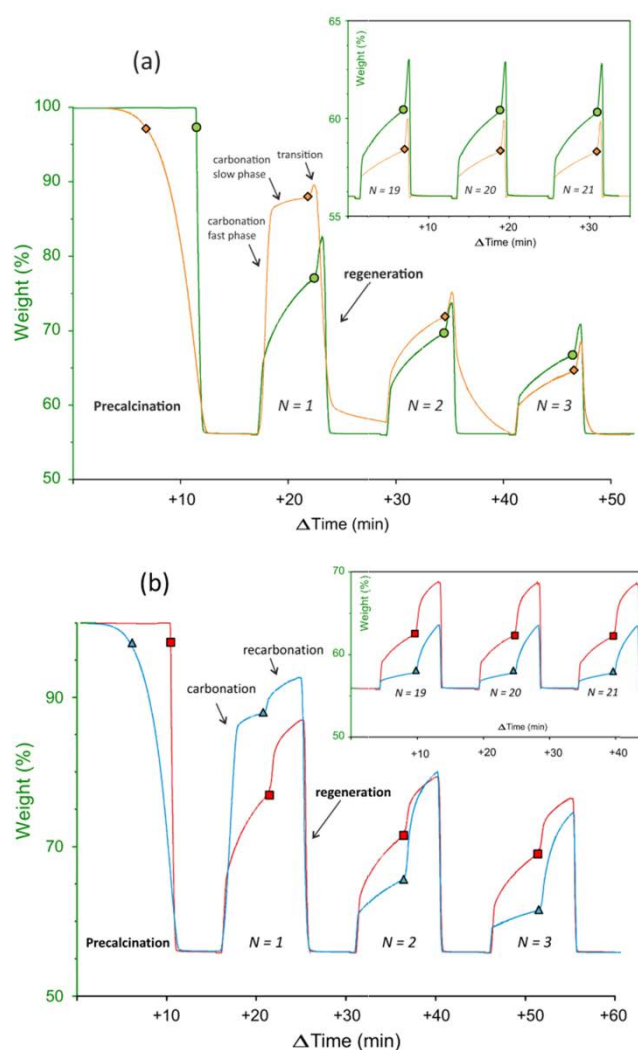
927 The CaO derived from precalcination at 950°C under high CO₂ concentration presents a low
 928 conversion in the first cycle as compared to the CaO obtained from precalcination in air, which
 929 has a higher porosity. Moreover, it is clear from Figure 7 that precalcination conditions have an
 930 important influence on the multicyclic behavior of the sorbent. The sample precalcined in air
 931 presents a drastic drop of conversion after the first cycle,⁸⁹ whereas the conversion of the sample
 932 precalcined under high CO₂ concentration decays at a lower rate. Consequently, conversion of
 933 the latter is higher from the fourth cycle. While Equation 1 is not able to provide a good fit to
 934 the conversion data of the sorbent precalcined in air, the sample precalcined under high CO₂
 935 concentration is well fitted by this equation yielding a residual value of 0.079, which is similar
 936 to the residual value of conversion for samples regenerated under low CO₂ partial pressure. Yet,
 937 regeneration under CO₂ yields a larger deactivation rate.



949
 950 Figure 7. CaO conversion at the end of the carbonation stage (X_N) as a function of the cycle number (N)
 951 for samples of raw limestone subjected to carbonation/calcination (carb/cal) and
 952 carbonation/recarbonation/calcination (carb/recarb/cal) cycles. Precalcination and regeneration conditions
 953 are indicated. The solid lines are the best fits from Eq. (1). Reproduced with permission from reference
 954 [25]. Copyright 2014. Applied Energy.

955
 956
 957 Figure 7 also shows the effect of introducing a recarbonation stage aimed at reactivating the
 958 sorbent. In carb/recarb/cal cycles, 3 minutes of recarbonation in 10% air and 90% CO₂ (vol/vol)
 959 at 800°C were introduced between the carbonation and the calcination stages.²⁵ Interestingly, the
 960 effect of recarbonation depends on the precalcination stage. Thus, the recarbonation stage
 961 accentuates the drop of CaO conversion if precalcination is performed in air. On the other hand,
 962 recarbonation improves the conversion of the sample precalcined under high CO₂ concentration,
 963 with an enhanced residual conversion, obtained fitting the data with Equation 1, of $X_r=0.131$.

964 Thermograms corresponding to the different experiments above reviewed are shown in Figure
 965 8. The higher conversion of the CaO precalcined in air in the first cycle, as observed in Figure 7,
 966 is due to its high reactivity in the fast carbonation phase, and its drastic drop in conversion can
 967 be associated to the high susceptibility of the soft CaO skeleton resulting from precalcination in
 968 air to sintering. On the other hand, the low reactivity in the first cycle of the CaO obtained from
 969 precalcination under high CO₂ concentration is explained by the enhancement of sorbent
 970 sintering under these conditions. However, precalcination under CO₂ mitigates the subsequent
 971 reduction of the CaO surface available for reaction.^{109, 110} As stated above, the carbonation stage
 972 is seen to take place through two phases,¹¹¹ a reaction controlled phase on the surface of the
 973 CaO particles and a slower phase controlled by the solid-state diffusion of CO₂ into the
 974 material.^{112, 113}



996 Figure 8. Time evolution of sorbent weight% during precalcination and the three first and last (inset)
 997 cycles for raw limestone. (a) Carbonation/calcination cycles of limestone slowly precalcined at 850°C in
 998 air (orange line) and quickly precalcined at 950°C under 70% CO₂ (green line). (b)
 999 Carbonation/recarbonation/calcination cycles of limestone precalcined at 850°C in air (blue line) and at
 1000 950°C under 70% CO₂ (red line). Carbonation at 650°C for 5 min (15% CO₂/85% air vol/vol), calcination
 1001 (regeneration) for 5 min at 950°C (70% CO₂/30% air vol/vol). Reproduced with permission from
 1002 reference [25]. Copyright 2014. Applied Energy.

1003 Note also in the thermograms shown in Figure 8a that carbonation in the diffusion controlled
 1004 phase of the 1st cycle for the sample precalcined in air is negligible as compared to carbonation
 1005 in the fast kinetically controlled phase. On the contrary, the diffusion controlled phase gains an
 1006 extraordinary relevance after regeneration under high CO₂ concentration.

1007 A similar behavior is observed in the thermograms of the carb/recarb/cal experiments shown in
 1008 Figure 8b. Thus, diffusion controlled carbonation and recarbonation in the first cycle is more
 1009 marked for the sample precalcined under high CO₂ concentration. As may be seen, the
 1010 carbonation reactivity of the sample precalcined in air is severely reduced after only few cycles.
 1011 A possible mechanism proposed for product layer formation and growth establishes that CaCO₃
 1012 nucleates on CaO surface in islands with a critical size which depends on temperature controlled
 1013 surface diffusion.^{114, 115} Surface diffusion is considerable when the temperature is close to the
 1014 Huttig temperature, T_H ≈ 690°C for CaO and T_H ≈ 260°C for CaCO₃. Thus, the intense
 1015 carbonation observed in the recarbonation stage can be explained due to the high surface
 1016 diffusion controlled reactivity at 800°C and 90% CO₂ in vol.

1017 Figure 9 illustrates SEM micrographs of samples subjected to 20 cycles under different
 1018 precalcination and regeneration conditions. Thus, samples precalcined in air and regenerated
 1019 under 70% CO₂ (Figure 9a), with very low CaO conversion, show large grains as compared
 1020 with the grain size of the samples precalcined and regenerated under high CO₂ concentration
 1021 (Figure 9b). Among these samples, those subjected to the intermediate recarbonation stage
 1022 present smaller grain size (Figure 9c) than those subjected to carb/cal cycles. It may be seen that
 1023 the CaO grains have a characteristic size that depends on the conditions of the experiments. CaO
 1024 conversion in the fast kinetically controlled phase depends on the available surface area for
 1025 carbonation and is therefore inversely correlated to grain size as shown in a recent work.¹⁰⁸

1026

1027

1028

1029

1030

1031

1032

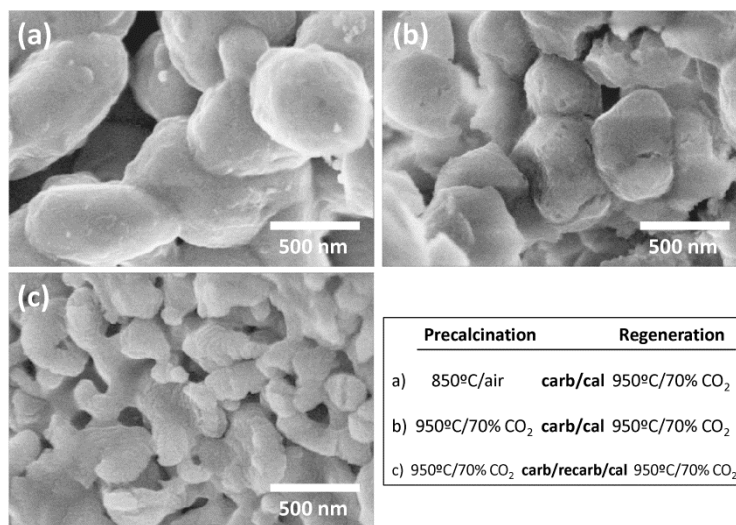
1033

1034

1035

1036

1037



1038

1039

1040

Figure 9. SEM pictures of limestone samples after being subjected to 20 carb/cal (a and b) and carb/recarb/cal cycles (c) under different precalcination and regeneration (calcination) conditions as indicated. Reproduced with permission from reference [25]. Copyright 2014. Applied Energy.

1041 **8. The multicyclic CO₂ capture capacity of natural dolomites at CaL conditions**

1042

1043 Dolomite, CaCO₃•MgCO₃, is another natural and abundantly available material that has been
1044 considered as CaO precursor for the CaL technology.^{4, 29, 116} Dolomite has a relatively lower
1045 stoichiometric capture capacity because carbonation of MgO is not thermodynamically
1046 favorable at CaL conditions.^{4, 117} However, the irreversible decomposition of MgCO₃ that takes
1047 place during precalcination yields stable MgO inert nanograins that would serve to increase the
1048 available CaO surface area of the calcined sorbent thus favoring the CaO reactivity.¹¹⁸
1049 Moreover, due to its high resistance to sintering at high temperatures, the presence of inert MgO
1050 nanograins in calcined dolomite would increase the thermal stability of the sorbent, although the
1051 detailed mechanism of thermal decomposition of dolomite is still unclear.¹¹⁹⁻¹²¹ Despite the
1052 potential advantages of using dolomite, experimental measurements reported in literature
1053 generally fail to show a superior performance of dolomite as compared to limestone. Yet, most
1054 lab-scale tests on dolomite or CaO•MgO synthetic composites do not mimic realistic CaL
1055 conditions.¹²²⁻¹²⁵ The multicyclic capture performance of dolomite and limestone has been
1056 recently compared in TGA tests reproducing severe calcination conditions (950°C, 70% CO₂
1057 vol.). This work has shown that the sorbent derived from dolomite does have a higher residual
1058 capture capacity than CaO derived from limestone despite of the lower CaO content of
1059 dolomite.¹²⁶

1060 In order to assess the performance of dolomite as a suitable sorbent in the CaL technology for
1061 practical purposes, the presence of inert MgO in dolomite has to be taken into account. For this
1062 reason, the capture capacity, defined as the ratio of mass of CO₂ captured to the mass of sorbent
1063 before each carbonation stage (including both CaO and MgO for dolomite), is the appropriate
1064 parameter to be studied in a comparative analysis with limestone.⁹¹ Figure 10a presents
1065 multicyclic capture capacity results from carb/cal test in which dolomite and limestone samples
1066 were precalcined in air and regenerated under high CO₂ concentration. As shown above in terms
1067 of conversion (Figure 7), CaO derived from limestone suffers a drastic drop of its capture
1068 capacity after regeneration. Dolomite however deactivates at a lower rate and after 20 cycles its
1069 capture capacity is almost twice that of limestone. Moreover, while limestone is affected by
1070 precalcination conditions, and recarbonation is detrimental for limestone precalcined in air
1071 (Figure 7), recarbonation does not produce an appreciable effect on the performance of
1072 dolomite. In general, the multicyclic behavior of dolomite is not significantly sensitive to the
1073 conditions of precalcination, even when precalcination conditions are severe (Figure 10b),
1074 which makes it rather predictable regardless of precalcination conditions. Only if limestone is
1075 precalcined under severe conditions (involving high CO₂ concentration) and subjected to
1076 recarbonation, its capture capacity may evolve similarly to that of dolomite (see Figures 7 and
1077 10b). These results strongly suggest that natural dolomite would improve the CO₂ capture

1078 efficiency at least to the same extent than the introduction of a recarbonator would do when
 1079 using limestone.

1080

1081

1082

1083

1084

1085

1086

1087

1088

1089

1090

1091

1092

1093

1094

1095

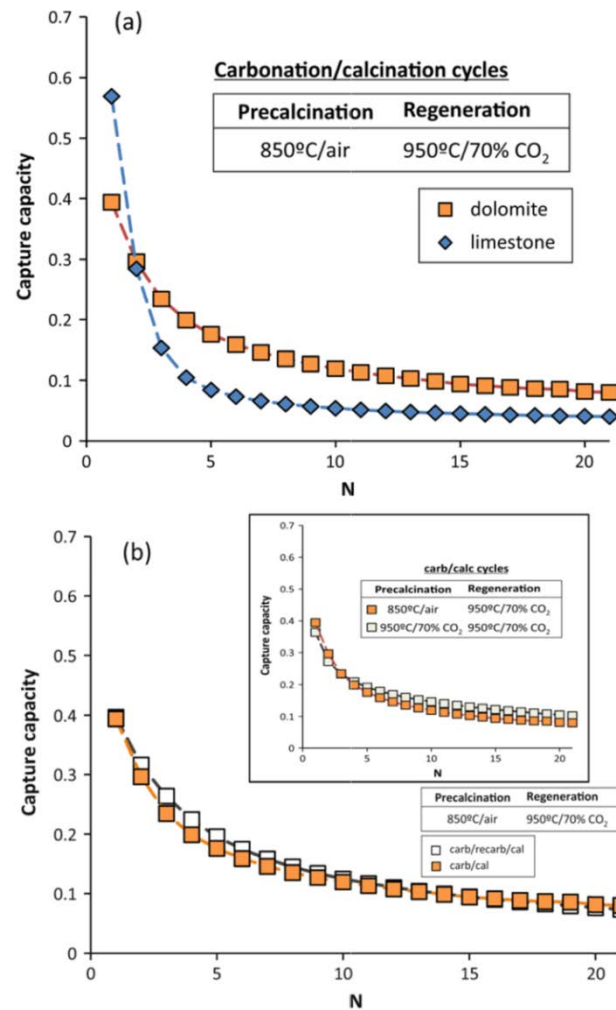
1096

1097

1098

1099

1100



1101 Figure 10. (a) CO₂ capture capacity as a function of carb/cal cycle number for dolomite and limestone
 1102 samples precalcined in air and regenerated by calcination in 70%CO₂ at 950°C. (b) CO₂ capture capacity
 1103 as a function of cycle number for dolomite samples subjected to carb/cal and carb/recarb/cal cycles
 1104 precalcined in air and regenerated by calcination under 70%CO₂ at 950°C. The inset shows the CO₂
 1105 capture capacity for dolomite precalcined under different conditions and subjected to carb/cal cycles,
 1106 calcined at 950°C in 70% CO₂. Reproduced with permission from reference [91]. Copyright 2015.
 1107 Applied Energy.

1108

1109 Figure 11a illustrates SEM micrographs of dolomite samples precalcined in air and subjected to
 1110 carb/cal cycles under severe regeneration conditions. Remarkably, these samples show a higher
 1111 porosity than limestone samples subjected to the same conditions (Figure 9). Individual MgO
 1112 grains, with a size of about 100 nm, can be clearly observed, dispersed in the sintered CaO.
 1113 Thus, the enhanced porosity and thermal stability provided by the MgO skeleton could be the
 1114 responsible mechanism for the high capture capacity of dolomite in comparison with limestone.
 1115 Note that a marked segregation of the MgO nanograins from the sintered CaO skeleton can be

1116 observed for dolomite samples subjected to carb/recarb/cal cycles precalcined and regenerated
1117 in severe conditions (Figure 11b). Taken into account that diffusivity is enhanced by the
1118 recarbonation conditions,¹²⁷⁻¹²⁹ the segregation of MgO and CaO grains would be expected to be
1119 promoted, in agreement with in situ observations.¹²¹ This phenomenon causes a slight decrease
1120 in capture capacity of dolomite precalcined under severe calcination conditions when the
1121 intermediate recarbonation stage is introduced.

1122

1123

1124

1125

1126

1127

1128

1129

1130

1131

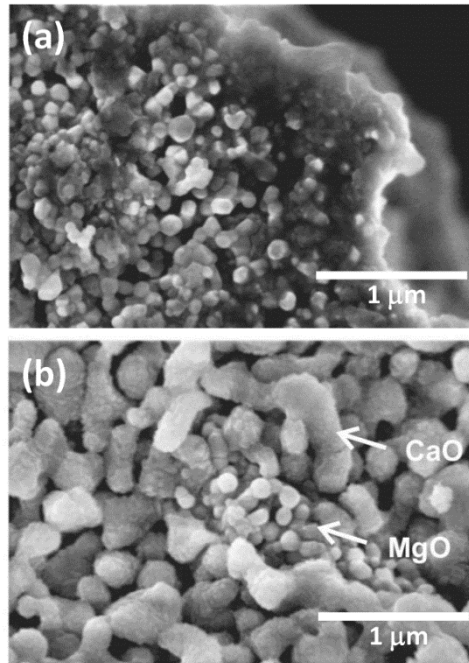
1132

1133

1134

1135

1136



1137 Figure 11. SEM pictures of dolomite samples (a) after being subjected to carb/cal cycles (precalcined at
1138 850°C in air and regenerated by calcination in 70% CO₂ at 950°C and (b) after being subjected to
1139 carb/recarb/cal cycled precalcined and regenerated by calcination under 70% CO₂ at 950°C. Reproduced
1140 with permission from reference [91]. Copyright 2015. Applied Energy.

1141

1142 A further benefit of using dolomite instead of limestone in the CaL technology would be the
1143 possibility of reducing the calcination temperature. Figure 12 illustrates the kinetics of
1144 limestone calcination under 70% vol CO₂ by quickly increasing the temperature up to 950°C.
1145 The presence of CO₂ hinders severely the decarbonation of limestone, as observed in many
1146 works.^{6, 107, 130-133} Not only the thermodynamic equilibrium is displaced to higher temperatures
1147 but also decarbonation of CaCO₃ is markedly slowed down. As may be seen in Figure 12,
1148 limestone decarbonation starts at about 900°C (30°C above the thermodynamic equilibrium
1149 temperature under 70% vol CO₂ at atmospheric pressure).⁶ The kinetics of dolomite calcination
1150 under 70% vol CO₂ shows different features as compared to limestone (Figure 13). Thus,
1151 decomposition of dolomite under high CO₂ concentration occurs in two stages.^{134, 135} In a first
1152 stage, irreversible MgCO₃ decomposition takes place, whereas the second stage, involving

1153 CaCO_3 decomposition, is initiated at about 650°C , which is well below the equilibrium
 1154 temperature for pure CaCO_3 decomposition. Moreover, decarbonation of dolomite is complete
 1155 in less than 5 min at 900°C . The two stages calcination of dolomite in environments of high CO_2
 1156 partial pressure has been widely reported in literature, but the mechanism of the reactions
 1157 involved is still under debate.^{91, 119-122, 135, 136}

1158

1159

1160

1161

1162

1163

1164

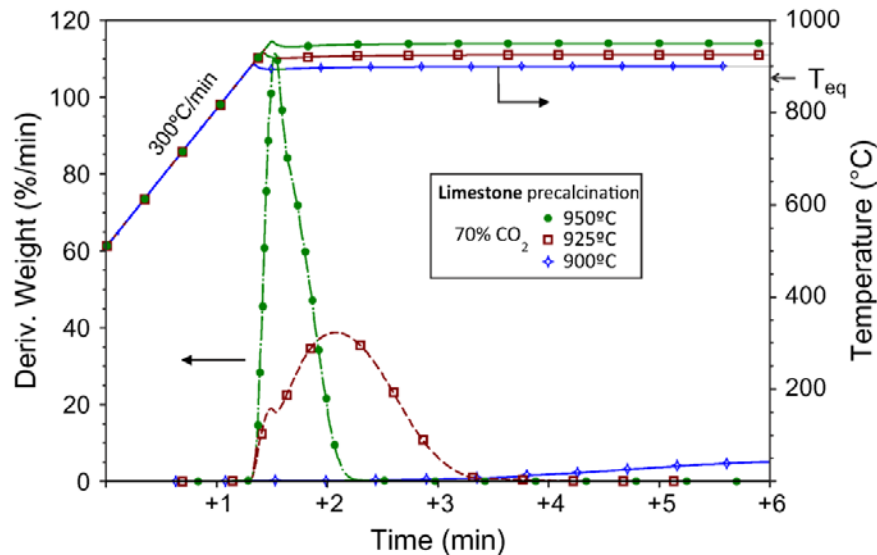
1165

1166

1167

1168

1169



1170

1171

1172

1173

1174

1175

Figure 12. Time evolution of sample weight % derivative (absolute value) and temperature during decomposition of samples of limestone precalcined in-situ in the TGA tests under 70% CO_2 by quickly increasing the temperature up to 900°C , 925°C , and 950°C (as indicated). The arrow in the temperature axis (right) indicates the thermodynamic equilibrium temperature ($T_{\text{eq}} \approx 870^\circ\text{C}$). Reproduced with permission from reference [91]. Copyright 2015. Applied Energy.

1176

1177

1178

1179

1180

1181

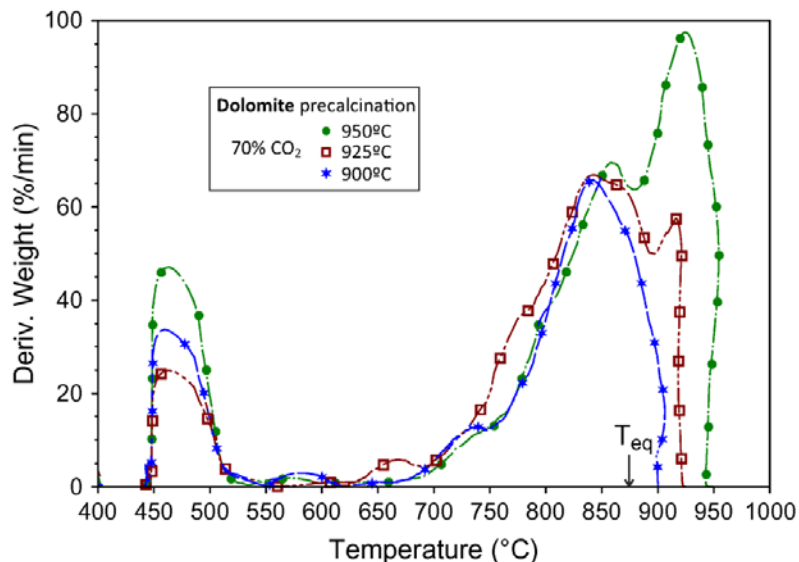
1182

1183

1184

1185

1186



1187

1188

1189

1190

1191

1192

Figure 13. Derivative of sample weight % (absolute value) as a function of temperature during decomposition of samples of dolomite precalcined under 70% vol CO_2 in the TGA tests by quickly increasing the temperature up to 900°C , 925°C , and 950°C (as indicated). The arrow in the temperature axis (horizontal) indicates the thermodynamic equilibrium temperature for calcite ($T_{\text{eq}} \approx 870^\circ\text{C}$). Reproduced with permission from reference [91]. Copyright 2015. Applied Energy.

1193 Some authors have shown experimentally that the capture capacity of dolomite is lower than
1194 that of limestone from the first carbonation/calcination cycles. However, most of these tests
1195 have been carried out at conditions far from realistic. On the other hand, it has been recently
1196 demonstrated that dolomite has a superior capture capacity (which also takes into account the
1197 inert MgO) as compared to limestone at realistic CaL conditions (implying high CO₂
1198 concentration, high temperature for calcination and quick transitions between carbonation and
1199 calcination stages).⁹¹ Moreover, the capture capacity of limestone derived CaO is critically
1200 influenced by the conditions of precalcination and the inclusion or not of a recarbonation stage,
1201 while the behavior of the sorbent derived from dolomite is almost insensitive to precalcination
1202 and recarbonation conditions, which allow predicting the dolomite behavior on a more solid
1203 basis. The improved stability provided by the inert MgO skeleton, as stated above, is thought to
1204 enhance the multicyclic capture capacity of dolomitic CaO at realistic CaL conditions.. In
1205 addition, an further advantage of the use of dolomite would be its fast decomposition under CO₂
1206 that would allow reducing the temperature of the calciner, which is the main energy penalty of
1207 the CaL technology.As regards the decomposition enthalpies of limestone and dolomite, they
1208 are 1.78 kJ g⁻¹ and 1.63 kJ g⁻¹, respectively. Therefore, the use of dolomite in the CaL process
1209 would imply also a lower energy consumption in the calciner, where the main energy penalty to
1210 the technology is imposed. Moreover, differential thermal analysis (DTA) experiments have
1211 shown that the enthalpy to decompose dolomite can be reduced by mechanical milling, which is
1212 an industrial scalable process.¹³⁷

1213

1214

1215 **9. Effect of thermal pretreatment of limestone on its multicyclic CO₂ capture behavior**

1216

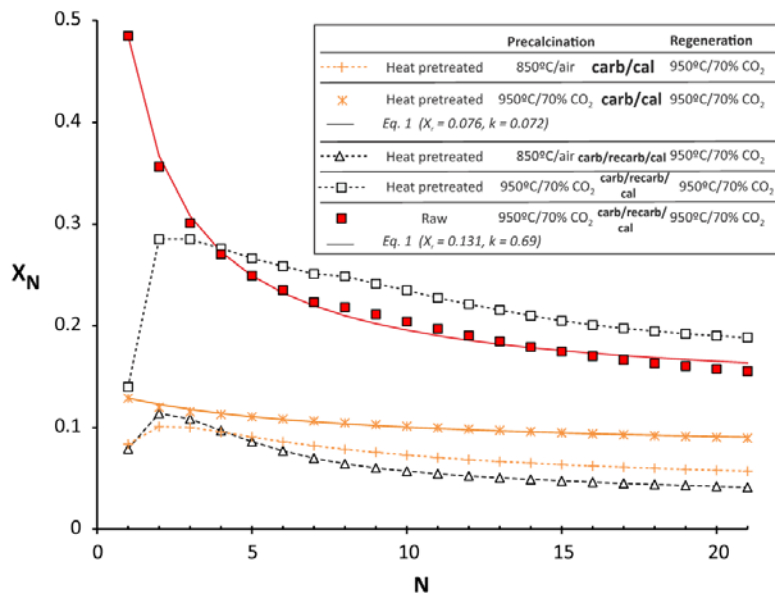
1217 Prolonged heating of the sorbent at high temperatures prior to its use in the CaL process was
1218 proposed as a feasible technique to improve the multicyclic conversion of CaO by Manovic and
1219 Anthony,⁹⁸ who observed a positive effect of thermal pretreatment on the multicyclic CO₂
1220 capture behavior of CaO.¹³⁸⁻¹⁴⁰ Recrystallization of CaO during thermal pretreatment, which
1221 leads to a hard stable porous skeleton, was proposed as the main cause of the high efficiency of
1222 the pretreatments on reactivation of the sorbent, especially under CO₂ enriched atmosphere.¹³⁹
1223 Thus, experimental results showed that the capture capacity of the pretreated sorbent, although
1224 small in the first cycle, was in fact increased with the cycle number during the first 10-20 cycles
1225 up to reach a stable value over the residual capture capacity of non-pretreated natural limestone.
1226 Moreover, another advantage of thermal pretreatment would be the increase in the mechanical
1227 strength of the sorbent. The effect of thermal pretreatment became however a controverted issue
1228 since initial TGA tests carried out to show reactivation were not carried out at realistic CaL
1229 conditions. Reactivation was enhanced by the regeneration conditions applied, which involved

1230 relatively low temperatures and low CO₂ partial pressures.⁹⁸ Further carbonation/calcination
 1231 tests carried out by calcination at temperatures above 900°C failed to confirm sorbent
 1232 reactivation.^{98, 141}

1233 Figure 14 compares multicyclic CaO conversion data obtained for samples of heat pretreated
 1234 (isothermal preheating in air at 950°C for 12 h) and raw limestone subjected to carb/calc and
 1235 carb/recarb/cal cycles in which sorbent regeneration is carried out at 950°C under 70% vol CO₂.
 1236 In carb/calc tests, heat pretreatment does not yield reactivation, and conversion after the first
 1237 cycle is maintained at a small value. Equation 1 is able to fit the conversion data and a value of
 1238 residual conversion is similar to that of raw limestone tested under the same conditions, with the
 1239 disadvantage that conversion of the first cycle is just about 0.13. An even bigger drop of CaO
 1240 conversion is observed if the heat pretreated sample is precalcined in air. A different behavior is
 1241 observed when heat pretreatment, precalcination under high CO₂ concentration and
 1242 recarbonation are combined. Then, a significant reactivation of CaO conversion is obtained
 1243 from the second carb/recarb/cal cycle for the heat pretreated sample, which becomes higher than
 1244 that of raw limestone subjected to carb/recarb/cal cycles under the same conditions and remains
 1245 higher with the number of cycles. Thus, the synergistic combination of heat pretreatment and
 1246 recarbonation improves the multicyclic CaO conversion when precalcination and regeneration
 1247 are performed under high CO₂ concentration.

1248
 1249
 1250
 1251
 1252
 1253
 1254
 1255
 1256
 1257
 1258

1259
 1260
 1261
 1262
 1263
 1264
 1265
 1266
 1267
 1268
 1269
 1270



1271
1272
1273
1274
1275
1276
1277
1278
1279
1280
1281

Fig. 14. CaO conversion at the end of the carbonation stage (X_N) as a function of the cycle number (N) for samples of heat pretreated and raw limestone subjected to carb/cal and carb/recarb/calc cycles. Carbonation at 650°C for 5 min (15% CO₂/85% air vol/vol), calcination (regeneration) for 5 min at 950°C (70% CO₂/30% air vol/vol) and recarbonation at 800°C for 3 min (90% CO₂/10% air vol/vol). Different precalcination conditions are indicated. The solid lines are the best fits from Eq. (1). Reproduced with permission from reference [25]. Copyright 2014. Applied Energy.

1282

1283 10. Effect of mechanical pretreatment of limestone on its multicyclic CO₂ capture behavior

1284

1285 Mechanical milling is a common treatment used in the industry to favor chemical reactions by
1286 creating a high density of structural defects in the solid crystal structure, which serves to
1287 enhance solid-state diffusion.¹⁴²⁻¹⁴⁴ The milling method to prepare materials with reduced
1288 crystallinity and enhanced reactivity is simple, relative inexpensive and is applicable to almost
1289 all kind of materials, with the possibility of scaling up to tonnage quantities of materials.¹⁴⁵⁻¹⁴⁷

1290 Figure 15 shows the time evolution of sorbent weight % during carbonation/calcination cycles
1291 for samples of raw, milled, and annealed limestone. Limestone was milled in a centrifugal mill
1292 (working at 500 rpm) employing 100 cm³ steel jar with 200 tungsten carbide balls 5.5 mm in
1293 diameter, and a sample-to-ball mass ratio of 1:40.¹²⁹ Thermal annealing was pursued by
1294 subjecting a limestone sample to a pure CO₂ atmosphere at 850°C for 12 h.

1295

1296

1297

1298

1299

1300

1301

1302

1303

1304

1305

1306

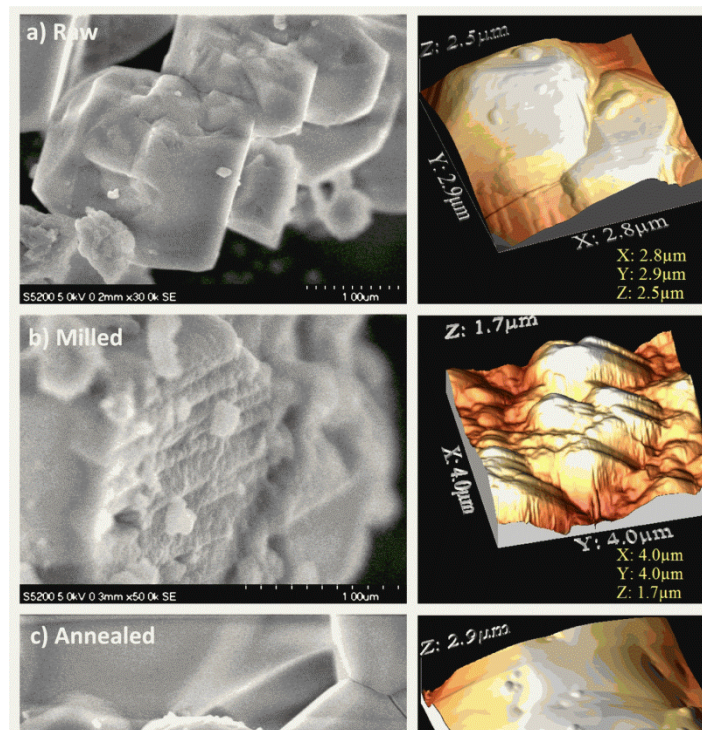
1307

1308

1309

1310

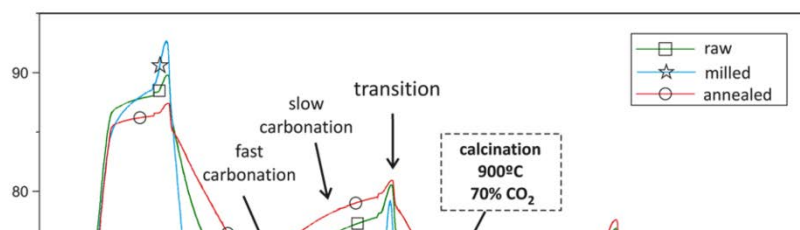
1311



1312
1313
1314
1315
1316
1317
1318
1319
1320
1321
1322
1323
1324
1325
1326
1327
1328
1329
1330
1331
1332
1333
1334
1335
1336
1337
1338
1339
1340
1341
1342
1343
1344
1345
1346
1347
1348
1349
1350

Figure 15. Scanning electron microscopy (SEM) and 3D scanning probe microscope (SPM) images of limestone particles from raw (a), milled (b) and thermally annealed (c) samples. SEM analysis was made by using a HITACHI Ultra High-Resolution S-5200 equipment. SPM images were obtained by using a Molecular Imaging Pico Plus system provided with AppNano ACT silicon tapping-mode rectangular cantilevers. Reproduced with permission from reference [126]. Copyright 2014. Environmental Science and Technology.

The increase of crystallinity degree induced by annealing enhances the resistance to solid-state diffusion thus playing the opposite role of milling.^{148, 149} Figure 15 shows scanning electron (SEM) and scanning probe microscopy (SPM) images which demonstrate contrasting effects of milling and thermal annealing on the structure of the solids. In the milled particles, the structural damage is clearly appreciable, while the surface of the annealed particles appears smoothed. In the carb/cal tests carried out to assess the effect of crystal structure sorbent regeneration was carried out by calcination under 70% CO₂ at 900°C whereas the samples were precalcined in air. As can be seen, most carbonation in the first cycle occurs through the kinetically controlled fast phase and up to a similar extent for the three samples. Once the fast carbonation phase is ended, CaO conversion is controlled by diffusion and would be inversely correlated to CaO crystallite size.¹⁵⁰ In accordance to the expected effects of pretreatment on the crystallinity of the solids, it is seen in Figure 16 that carbonation in the diffusion-controlled phase is enhanced for the milled sample while annealing hinders it. This behavior is more apparent in the short transition between carbonation and calcination. The sharp overshoot observed in the weight gain is due to the enhancement of carbonation when CO₂ concentration is increased from 15% vol to 70% vol and until the equilibrium temperature is reached. Since surface diffusion becomes noticeable at temperatures close to the Huttig temperature, it would be promoted at high temperatures by structural defects that enhance the exposition of surface available in the sorbent for accelerated recarbonation in the transitory period.¹²⁹ Although the critical temperature for decarbonation under 70% vol CO₂ is about 870°C,⁶ it may be seen in Figure 15 that calcination at 900°C does not yield a sufficiently fast regeneration of CaO derived from raw limestone.



1351
1352
1353
1354
1355
1356
1357
1358
1359
1360
1361
1362
1363
1364
1365
1366
1367
1368
1369
1370
1371
1372
1373
1374
1375
1376
1377
1378
1379
1380
1381
1382
1383
1384
1385
1386
1387
1388

Figure 16. Time evolution of sorbent weight % during carbonation/calcination cycles for samples of raw, milled and annealed limestones. Carbonation at 650 °C for 5 min (15% CO₂/85% air vol/vol). Calcination for 5 min at 900 °C (70% CO₂/30% air vol/vol). Reproduced with permission from reference [126]. Copyright 2014. Environmental Science and Technology.

Decarbonation is even slower for the annealed sample with a higher crystallinity. On the other hand, decarbonation is fast and completed at 900°C for the sorbent derived from milled limestone. The limiting mechanism of calcination under these conditions involving CO₂ desorption and structural transformation step would be enhanced by the structural damage caused by milling.^{107, 116, 130, 132, 133}

A straightforward recommendation that may be extracted from this study is that the use of limestone with low crystallinity should be pursued in favor of highly crystalline solids. This would allow for a reduction of the calciner temperature of about 50°C while maintaining high calcination efficiency.

Natural chalk, whose chemical composition is mainly CaCO₃ with minor presence of silt and clay, has been proposed also as a natural CaO precursor to be used in the CaL process not just for carbonation but also for SO₂ removal¹⁵¹. CO₂ capture capacity and uptake of SO₂ were compared with that of limestone and dolomite in a fluidized bed. The sulfation was carried out at 850°C in 0.18 vol% SO₂ and 5.2 vol% O₂ (N₂ balance) and the CO₂-capture tests were performed at 750°C with calcination in pure N₂ followed by carbonation in 14 vol % CO₂ (N₂ balance).¹⁵¹ Under these conditions, the uptake of SO₂ and CO₂ capture of chalk derived CaO were higher than those of limestone and dolomite derived CaO . A subject of great interest to be analyzed in future works would be whether natural chalk still maintains a superior capture performance as compared to limestone and dolomite under the severe calcination conditions typical of the CaL process.

1389 **11. Pilot-plant testing**

1390

1391 Demonstration of the CaL technology in pilot-scale plants is required to optimize the process
1392 parameters and has been in fact one of the most significant fields of advancement of the
1393 technology. A number of test facilities have been built worldwide in the last five years. The
1394 interested reader on pilot-plant testing is referred to the very recently published Hanak's
1395 exhaustive review and references therein.¹⁵⁵ Here we give just a brief summary of the largest
1396 scale facilities that are currently demonstrating the efficiency of CO₂ capture by means of the
1397 CaL process.

1398 The pilot plant in La Pereda (Asturias, Spain) is a 1.7 MW_{th} facility designed to process
1399 approximately 1% of the flue gas produced in a 50 MW_{el} coal-fired commercial power plant.

1400 The pilot plant consists of two interconnected circulating fluidized bed (CFB) reactors operating
1401 at gas velocities of 3-5 m s⁻¹, with operating temperatures of 600-715°C for the carbonator and
1402 820-950°C for the calciner, which is fired with coal.⁸ The experimental facility at Darmstadt

1403 University of Technology is a 1MW_{th} pilot plant comprising two interconnected CFB reactors
1404 that are refractory lined. In this plant, the fresh limestone is pre-heated in the carbonator at
1405 650°C to minimize the fuel and oxygen consumption in the calciner. The fluidizing medium in
1406 the carbonator is a synthetic flue gas and oxygen-enriched air is used to fluidize the calciner.¹⁵²

1407 The Industrial Technology Research Institute in Taiwan has erected a 1.9 MW_{th} pilot plant,
1408 which is integrated into a cement plant that is able to remove a tonne of CO₂ per hour. The
1409 system contains a bubbling fluidized bed reactor, a gas distributor and a moving bed calciner.
1410 The temperature in the carbonator is controlled by water-cooled steel jackets and the heat for
1411 calcination is obtained by oxy-combustion of diesel.¹⁵³

1412 The CaL technology has also been integrated with biomass combustion. Thus, a 0.3 MW_{th} pilot
1413 plant has been developed to capture CO₂ during the combustion of biomass in a fluidized bed
1414 operating in continuous mode. The pilot plant is located at a 655 MW_e coal power plant in Leon
1415 (Spain) and operates at temperatures around 700°C both in the carbonator and in the calciner in
1416 order to maximize the combustion and CO₂ capture efficiencies. The use of biomass as a fuel in
1417 CCS systems (BIO-CSS) would allow producing power with negative emissions of CO₂¹⁵⁴. The
1418 necessity of urgently developing BIO-CCS technologies is increasingly gaining importance as
1419 perspectives of keeping CO₂ concentration in the atmosphere below 450ppm in order to limit
1420 global warming to +2°C from pre-industrial level are becoming more pessimistic.

1421

1422

1423 **12. Acknowledgements**

1424

1425 Financial support by the Spanish Government Agency Ministerio de Economía y
1426 Competitividad (contracts CTQ2014-52763-C2-2-R and CTQ2014-52763-C2-1-R) and
1427 Andalusian Regional Government (Junta de Andalucía-FEDER contracts FQM-5735 and TEP-
1428 7858) is acknowledged. The authors also thank VPPI-US for the AP current contract.

1429

1430

1431

1432 13. References

- 1433 1. Metz, B.; Davidson, O.; Coninck, H. D.; Loos, M.; Meyer, L., *Special report on carbon*
1434 *dioxide capture and storage, intergovernmental panel on climate change*, 2005.
- 1435 2. Middleton, R. S.; Eccles, J. K. The complex future of CO₂ capture and storage: Variable
1436 electricity generation and fossil fuel power. *Applied Energy* **2013**, 108, 66-73.
- 1437 3. Roddy, D. J. Development of a CO₂ network for industrial emissions. *Applied Energy*
1438 **2012**, 91, 459-465.
- 1439 4. Blamey, J.; Anthony, E. J.; Wang, J.; Fennell, P. S. The calcium looping cycle for large-
1440 scale CO₂ capture. *Progress in Energy and Combustion Science* **2010**, 36, 260-279.
- 1441 5. Romano, M. C. Modeling the carbonator of a Ca-looping process for CO₂ capture from
1442 power plant flue gas. *Chemical Engineering Science* **2012**, 69, 257-269.
- 1443 6. García-Labiano, F.; Abad, A.; de Diego, L. F.; Gayán, P.; Adánez, J. Calcination of
1444 calcium-based sorbents at pressure in a broad range of CO₂ concentrations. *Chemical*
1445 *Engineering Science* **2002**, 57, 2381-2393.
- 1446 7. Charitos, A.; Rodríguez, N.; Hawthorne, C.; Alonso, M.; Zieba, M.; Arias, B.; Kopanakis,
1447 G.; Scheffknecht, G.; Abanades, J. C. Experimental validation of the calcium looping
1448 CO₂ capture process with two circulating fluidized bed carbonator reactors. *Industrial*
1449 *& Engineering Chemistry Research* **2011**, 50, 9685-9695.
- 1450 8. Arias, B.; Diego, M. E.; Abanades, J. C.; Lorenzo, M.; Diaz, L.; Martínez, D.; Alvarez, J.;
1451 Sánchez-Biezma, A. Demonstration of steady state CO₂ capture in a 1.7 MWth calcium
1452 looping pilot. *International Journal of Greenhouse Gas Control* **2013**, 18, 237-245.
- 1453 9. Martínez, I.; Grasa, G.; Murillo, R.; Arias, B.; Abanades, J. C. Modelling the continuous
1454 calcination of CaCO₃ in a Ca-looping system. *Chemical Engineering Journal* **2013**, 215–
1455 216, 174-181.
- 1456 10. Kunze, C.; Spliethoff, H. Assessment of oxy-fuel, pre- and post-combustion-based
1457 carbon capture for future IGCC plants. *Applied Energy* **2012**, 94, 109-116.
- 1458 11. Lisbona, P.; Martínez, A.; Romeo, L. M. Hydrodynamical model and experimental
1459 results of a calcium looping cycle for CO₂ capture. *Applied Energy* **2013**, 101, 317-322.
- 1460 12. Romeo, L. M.; Lara, Y.; Lisbona, P.; Martínez, A. Economical assessment of competitive
1461 enhanced limestones for CO₂ capture cycles in power plants. *Fuel Processing*
1462 *Technology* **2009**, 90, 803-811.
- 1463 13. Ylätaalo, J.; Ritvanen, J.; Tynjälä, T.; Hyppänen, T. Model based scale-up study of the
1464 calcium looping process. *Fuel* **2014**, 115, 329-337.
- 1465 14. Chen, H.; Zhao, Z.; Huang, X.; Patchigolla, K.; Cotton, A.; Oakey, J. Novel optimized
1466 process for utilization of CaO-Based sorbent for capturing CO₂ and SO₂ sequentially.
1467 *Energy & Fuels* **2012**, 26, 5596-5603.
- 1468 15. Rodríguez, N.; Alonso, M.; Abanades, J. C.; Charitos, A.; Hawthorne, C.; Scheffknecht,
1469 G.; Lu, D. Y.; Anthony, E. J. Sulfation and reactivation characteristics of nine limestones.
1470 *Energy Procedia* **2011**, 4, 393-401.
- 1471 16. Sánchez-Biezma, A.; Ballesteros, J. C.; Diaz, L.; de Zárraga, E.; Álvarez, F. J.; López, J.;
1472 Arias, B.; Grasa, G.; Abanades, J. C. Postcombustion CO₂ capture with CaO. Status of

- 1473 the technology and next steps towards large scale demonstration. *Energy Procedia*
 1474 **2011**, 4, 852-859.
- 1475 17. Arias, B.; Abanades, J. C.; Grasa, G. S. Enhancement of fast CO₂ capture by a nano-
 1476 SiO₂/CaO composite at Ca-looping conditions. *Chemical Engineering Journal* **2011**, 167,
 1477 255–261.
- 1478 18. Martínez, A.; Lara, Y.; Lisbona, P.; Romeo, L. M. Operation of a cyclonic preheater in
 1479 the Ca-Looping for CO₂ capture. *Environmental Science & Technology* **2013**, 47, 11335-
 1480 11341.
- 1481 19. Rodriguez, N.; Alonso, M.; Grasa, G.; Abanades, J. C. Heat requirements in a calciner of
 1482 CaCO₃ integrated in a CO₂ capture system using CaO. *Chemical Engineering Journal*
 1483 **2008**, 138, 148-154.
- 1484 20. Romeo, L. M.; Lara, Y.; Lisbona, P.; Escosa, J. M. Optimizing make-up flow in a CO₂
 1485 capture system using CaO. *Chemical Engineering Journal* **2009**, 147, 252-258.
- 1486 21. Arias, B.; Grasa, G. S.; Alonso, M.; Abanades, J. C. Post-combustion calcium looping
 1487 process with a highly stable sorbent activity by recarbonation. *Energy & Environmental*
 1488 *Science* **2012**, 5, 7353-7359.
- 1489 22. Diego, M. E.; Arias, B.; Alonso, M.; Abanades, J. C. The impact of calcium sulfate and
 1490 inert solids accumulation in post-combustion calcium looping systems. *Fuel* **2013**, 109,
 1491 184-190.
- 1492 23. Grasa, G.; Martínez, I.; Diego, M. E.; Abanades, J. C. Determination of CaO carbonation
 1493 kinetics under recarbonation conditions. *Energy & Fuels* **2014**, 28, 4033-4042.
- 1494 24. Diego, M. E.; Arias, B.; Grasa, G.; Abanades, J. C. Design of a novel fluidized bed reactor
 1495 to enhance sorbent performance in CO₂ capture systems using CaO. *Industrial &*
 1496 *Engineering Chemistry Research* **2014**, 53, 10059-10071.
- 1497 25. Valverde, J. M.; Sanchez-Jimenez, P. E.; Perez-Maqueda, L. A. Role of precalcination
 1498 and regeneration conditions on postcombustion CO₂ capture in the Ca-looping
 1499 technology. *Applied Energy* **2014**, 136, 347-356.
- 1500 26. Chen, H.; Zhao, C.; Yang, Y.; Zhang, P. CO₂ capture and attrition performance of CaO
 1501 pellets with aluminate cement under pressurized carbonation. *Applied Energy* **2012**,
 1502 91, 334-340.
- 1503 27. Itskos, G.; Grammelis, P.; Scala, F.; Pawlak-Kruczek, H.; Coppola, A.; Salatino, P.;
 1504 Kakaras, E. A comparative characterization study of Ca-looping natural sorbents.
 1505 *Applied Energy* **2013**, 108, 373-382.
- 1506 28. Sun, R.; Li, Y.; Liu, H.; Wu, S.; Lu, C. CO₂ capture performance of calcium-based sorbent
 1507 doped with manganese salts during calcium looping cycle. *Applied Energy* **2012**, 89,
 1508 368-373.
- 1509 29. Valverde, J. M. Ca-based synthetic materials with enhanced CO₂ capture efficiency.
 1510 *Journal of Materials Chemistry A* **2013**, 1, 447-468.
- 1511 30. Abanades, J. C.; Anthony, E. J.; Wang, J. S.; Oakey, J. E. Fluidized bed combustion
 1512 systems integrating CO₂ capture with CaO. *Environmental Science & Technology* **2005**,
 1513 39, 2861-2866.
- 1514 31. Lisbona, P.; Romeo, L. M. Enhanced coal gasification heated by unmixed combustion
 1515 integrated with an hybrid system of SOFC/GT. *International Journal of Hydrogen*
 1516 *Energy* **2008**, 33, 5755-5764.
- 1517 32. Alonso, M.; Diego, M. E.; Pérez, C.; Chamberlain, J. R.; Abanades, J. C. Biomass
 1518 combustion with in situ CO₂ capture by CaO in a 300 kWth circulating fluidized bed
 1519 facility. *International Journal of Greenhouse Gas Control* **2014**, 29, 142-152.
- 1520 33. MacKenzie, A.; Granatstein, D. L.; Anthony, E. J.; Abanades, J. C. Economics of CO₂
 1521 capture using the calcium cycle with a pressurized fluidized bed combustor. *Energy &*
 1522 *Fuels* **2007**, 21, 920-926.
- 1523 34. Martínez, A.; Lara, Y.; Lisbona, P.; Romeo, L. M. Energy penalty reduction in the
 1524 calcium looping cycle. *International Journal of Greenhouse Gas Control* **2012**, 7, 74-81.

- 1525 35. Rodriguez, N.; Alonso, M.; Grasa, G.; Abanades, J. C. Heat requirements in a calciner of
1526 CaCO₃ integrated in a CO₂ capture system using CaO. *Chemical Engineering Journal*
1527 **2008**, 138, 148-154.
- 1528 36. Martínez, A.; Lara, Y.; Lisbona, P.; Romeo, L. M. Operation of a mixing seal valve in
1529 calcium looping for CO₂ capture. *Energy & Fuels* **2014**, 28, 2059-2068.
- 1530 37. Kim, K.; Kim, D.; Park, Y.-K.; Lee, K. S. A solid sorbent-based multi-stage fluidized bed
1531 process with inter-stage heat integration as an energy efficient carbon capture
1532 process. *International Journal of Greenhouse Gas Control* **2014**, 26, 135-146.
- 1533 38. Le Moullec, Y.; Neveux, T.; Al Azki, A.; Chikukwa, A.; Hoff, K. A. Process modifications
1534 for solvent-based post-combustion CO₂ capture. *International Journal of Greenhouse*
1535 *Gas Control* **2014**, 31, 96-112.
- 1536 39. Yin, J.; Qin, C.; Feng, B.; Ge, L.; Luo, C.; Liu, W.; An, H. Calcium looping for CO₂ capture
1537 at a constant high temperature. *Energy & Fuels* **2014**, 28, 307-318.
- 1538 40. Ball, R. Entropy generation analyses of Endex and conventional calcium looping
1539 processes for capture. *Fuel* **2014**, 127, 202-211.
- 1540 41. Yin, J.; Qin, C.; An, H.; Liu, W.; Feng, B. High-temperature pressure swing adsorption
1541 process for CO₂ separation. *Energy & Fuels* **2012**, 26, 169-175.
- 1542 42. Ball, R.; Sceats, M. G. Separation of carbon dioxide from flue emissions using Endex
1543 principles. *Fuel* **2010**, 89, 2750-2759.
- 1544 43. Ball, R. Using the second law first: Improving the thermodynamic efficiency of carbon
1545 dioxide separation from gas streams in an Endex calcium looping system. *Applied*
1546 *Thermal Engineering* **2015**, 74, 194-201.
- 1547 44. Romeo, L. M.; Abanades, J. C.; Escosa, J. M.; Paño, J.; Giménez, A.; Sánchez-Biezma, A.;
1548 Ballesteros, J. C. Oxyfuel carbonation/calcination cycle for low cost CO₂ capture in
1549 existing power plants. *Energy Conversion and Management* **2008**, 49, 2809-2814.
- 1550 45. Bugge, J.; Kjær, S.; Blum, R. High-efficiency coal-fired power plants development and
1551 perspectives. *Energy* **2006**, 31, 1437-1445.
- 1552 46. Hawthorne, C.; Trossmann, M.; Galindo Cifre, P.; Schuster, A.; Scheffknecht, G.
1553 Simulation of the carbonate looping power cycle. *Energy Procedia* **2009**, 1, 1387-1394.
- 1554 47. Romano, M. Coal-fired power plant with calcium oxide carbonation for
1555 postcombustion CO₂ capture. *Energy Procedia* **2009**, 1, 1099-1106.
- 1556 48. Yang, Y.; Zhai, R.; Duan, L.; Kavosh, M.; Patchigolla, K.; Oakey, J. Integration and
1557 evaluation of a power plant with a CaO-based CO₂ capture system. *International*
1558 *Journal of Greenhouse Gas Control* **2010**, 4, 603-612.
- 1559 49. Lisbona, P.; Martínez, A.; Lara, Y.; Romeo, L. M. Integration of carbonate CO₂ capture
1560 cycle and coal-fired power plants. A comparative study for different sorbents. *Energy*
1561 *& Fuels* **2010**, 24, 728-736.
- 1562 50. Martínez, I.; Murillo, R.; Grasa, G.; Carlos Abanades, J. Integration of a Ca looping
1563 system for CO₂ capture in existing power plants. *AIChE Journal* **2011**, 57, 2599-2607.
- 1564 51. Vorrias, I.; Atsonios, K.; Nikolopoulos, A.; Nikolopoulos, N.; Grammelis, P.; Kakaras, E.
1565 Calcium looping for CO₂ capture from a lignite fired power plant. *Fuel* **2013**, 113, 826-
1566 836.
- 1567 52. Lara, Y.; Lisbona, P.; Martínez, A.; Romeo, L. M. Design and analysis of heat exchanger
1568 networks for integrated Ca-looping systems. *Applied Energy* **2013**, 111, 690-700.
- 1569 53. Lara, Y.; Lisbona, P.; Martínez, A.; Romeo, L. M. A systematic approach for high
1570 temperature looping cycles integration. *Fuel* **2014**, 127, 4-12.
- 1571 54. Romeo, L. M.; Usón, S.; Valero, A.; Escosa, J. M. Exergy analysis as a tool for the
1572 integration of very complex energy systems: The case of carbonation/calcination CO₂
1573 systems in existing coal power plants. *International Journal of Greenhouse Gas Control*
1574 **2010**, 4, 647-654.

- 1575 55. Ströhle, J.; Galloy, A.; Epple, B. Feasibility study on the carbonate looping process for
1576 post-combustion CO₂ capture from coal-fired power plants. *Energy Procedia* **2009**, *1*,
1577 1313-1320.
- 1578 56. Wang, W.; Ramkumar, S.; Fan, L.-S. Energy penalty of CO₂ capture for the
1579 Carbonation–Calcination Reaction (CCR) process: Parametric effects and comparisons
1580 with alternative processes. *Fuel* **2013**, *104*, 561-574.
- 1581 57. Berstad, D.; Anantharaman, R.; Jordal, K. Post-combustion CO₂ capture from a natural
1582 gas combined cycle by CaO/CaCO₃ looping. *International Journal of Greenhouse Gas*
1583 *Control* **2012**, *11*, 25-33.
- 1584 58. Berstad, D.; Anantharaman, R.; Blom, R.; Jordal, K.; Arstad, B. NGCC post-combustion
1585 CO₂ capture with Ca/carbonate looping: Efficiency dependency on sorbent properties,
1586 capture unit performance and process configuration. *International Journal of*
1587 *Greenhouse Gas Control* **2014**, *24*, 43-53.
- 1588 59. Manovic, V.; Anthony, E. J. Integration of calcium and chemical looping combustion
1589 using composite CaO/CuO-Based materials. *Environmental Science & Technology* **2011**,
1590 *45*, 10750-10756.
- 1591 60. Ridha, F. N.; Lu, D.; Macchi, A.; Hughes, R. W. Combined calcium looping and chemical
1592 looping combustion cycles with CaO–CuO pellets in a fixed bed reactor. *Fuel* **2015**, *153*,
1593 202-209.
- 1594 61. Cormos, A.-M.; Simon, A. Assessment of CO₂ capture by calcium looping (CaL) process
1595 in a flexible power plant operation scenario. *Applied Thermal Engineering* **2015**, *80*,
1596 319-327.
- 1597 62. Harrison, D. P. Sorption-Enhanced hydrogen production: A review. *Industrial &*
1598 *Engineering Chemistry Research* **2008**, *47*, 6486-6501.
- 1599 63. Dean, C. C.; Blamey, J.; Florin, N. H.; Al-Jeboori, M. J.; Fennell, P. S. The calcium looping
1600 cycle for CO₂ capture from power generation, cement manufacture and hydrogen
1601 production. *Chemical Engineering Research and Design* **2011**, *89*, 836-855.
- 1602 64. Barelli, L.; Bidini, G.; Gallorini, F.; Servili, S. Hydrogen production through sorption-
1603 enhanced steam methane reforming and membrane technology: A review. *Energy*
1604 **2008**, *33*, 554-570.
- 1605 65. Lopez Ortiz, A.; Harrison, D. P. Hydrogen production using sorption-enhanced reaction.
1606 *Industrial & Engineering Chemistry Research* **2001**, *40*, 5102-5109.
- 1607 66. Connell, D. P.; Lewandowski, D. A.; Ramkumar, S.; Phalak, N.; Statnick, R. M.; Fan, L.-S.
1608 Process simulation and economic analysis of the Calcium Looping Process (CLP) for
1609 hydrogen and electricity production from coal and natural gas. *Fuel* **2013**, *105*, 383-
1610 396.
- 1611 67. Ramkumar, S.; Fan, L.-S. Calcium looping process (CLP) for enhanced noncatalytic
1612 hydrogen production with integrated carbon dioxide capture. *Energy & Fuels* **2010**, *24*,
1613 4408-4418.
- 1614 68. Florin, N. H.; Harris, A. T. Enhanced hydrogen production from biomass with in situ
1615 carbon dioxide capture using calcium oxide sorbents. *Chemical Engineering Science*
1616 **2008**, *63*, 287-316.
- 1617 69. Abanades, J. C.; Alonso, M.; Rodríguez, N.; González, B.; Grasa, G.; Murillo, R. Capturing
1618 CO₂ from combustion flue gases with a carbonation calcination loop. Experimental
1619 results and process development. *Energy Procedia* **2009**, *1*, 1147-1154.
- 1620 70. Siefert, N. S.; Chang, B. Y.; Litster, S. Exergy and economic analysis of a CaO-looping
1621 gasifier for IGFC–CCS and IGCC–CCS. *Applied Energy* **2014**, *128*, 230-245.
- 1622 71. Cormos, C.-C. Economic evaluations of coal-based combustion and gasification power
1623 plants with post-combustion CO₂ capture using calcium looping cycle. *Energy* **2014**, *78*,
1624 665-673.

- 1625 72. Cormos, C.-C. Economic implications of pre- and post-combustion calcium looping
1626 configurations applied to gasification power plants. *International Journal of Hydrogen*
1627 *Energy* **2014**, 39, 10507-10516.
- 1628 73. Xu, X.; Xiao, Y.; Qiao, C. System design and analysis of a direct hydrogen from coal
1629 system with CO₂ capture. *Energy & Fuels* **2007**, 21, 1688-1694.
- 1630 74. Moghtaderi, B. Review of the recent chemical looping process developments for novel
1631 energy and fuel applications. *Energy & Fuels* **2012**, 26, 15-40.
- 1632 75. Rahman, R. A.; Mehrani, P.; Lu, D. Y.; Anthony, E. J.; Macchi, A. Investigating the use of
1633 CaO/CuO sorbents for in situ CO₂ capture in a biomass gasifier. *Energy & Fuels* **2015**.
- 1634 76. Abanades, J. C.; Murillo, R.; Fernandez, J. R.; Grasa, G.; Martínez, I. New CO₂ capture
1635 process for hydrogen production combining ca and cu chemical loops. *Environmental*
1636 *Science & Technology* **2010**, 44, 6901-6904.
- 1637 77. Zhang, X.; Liu, Y. Performance assessment of CO₂ capture with calcination carbonation
1638 reaction process driven by coal and concentrated solar power. *Applied Thermal*
1639 *Engineering* **2014**, 70, 13-24.
- 1640 78. Edwards, S. E. B.; Materić, V. Calcium looping in solar power generation plants. *Solar*
1641 *Energy* **2012**, 86, 2494-2503.
- 1642 79. Sun, R.; Li, Y.; Liu, C.; Xie, X.; Lu, C. Utilization of lime mud from paper mill as CO₂
1643 sorbent in calcium looping process. *Chemical Engineering Journal* **2013**, 221, 124-132.
- 1644 80. Atsonios, K.; Grammelis, P.; Antiohos, S. K.; Nikolopoulos, N.; Kakaras, E. Integration of
1645 calcium looping technology in existing cement plant for CO₂ capture: Process modeling
1646 and technical considerations. *Fuel* **2015**, 153, 210-223.
- 1647 81. Ozcan, D. C.; Ahn, H.; Brandani, S. Process integration of a Ca-looping carbon capture
1648 process in a cement plant. *International Journal of Greenhouse Gas Control* **2013**, 19,
1649 530-540.
- 1650 82. Vatopoulos, K.; Tzimas, E. Assessment of CO₂ capture technologies in cement
1651 manufacturing process. *Journal of Cleaner Production* **2012**, 32, 251-261.
- 1652 83. Romeo, L. M.; Catalina, D.; Lisbona, P.; Lara, Y.; Martínez, A. Reduction of greenhouse
1653 gas emissions by integration of cement plants, power plants, and CO₂ capture systems.
1654 *Greenhouse Gases: Science and Technology* **2011**, 1, 72-82.
- 1655 84. Rodríguez, N.; Murillo, R.; Abanades, J. C. CO₂ capture from cement plants using
1656 oxyfired precalcination and/or calcium looping. *Environmental Science & Technology*
1657 **2012**, 46, 2460-2466.
- 1658 85. Romano, M. C.; Spinelli, M.; Campanari, S.; Consonni, S.; Marchi, M.; Pimpinelli, N.;
1659 Cinti, G. The calcium looping process for low CO₂ emission cement plants. *Energy*
1660 *Procedia* **2014**, 61, 500-503.
- 1661 86. Kuramochi, T.; Ramírez, A.; Turkenburg, W.; Faaij, A. Comparative assessment of CO₂
1662 capture technologies for carbon-intensive industrial processes. *Progress in Energy and*
1663 *Combustion Science* **2012**, 38, 87-112.
- 1664 87. Ylätaalo, J.; Parkkinen, J.; Ritvanen, J.; Tynjälä, T.; Hyppänen, T. Modeling of the oxy-
1665 combustion calciner in the post-combustion calcium looping process. *Fuel* **2013**, 113,
1666 770-779.
- 1667 88. Lu, D. Y.; Hughes, R. W.; Anthony, E. J.; Manovic, V. Sintering and reactivity of CaCO₃-
1668 based sorbents for in situ CO₂ capture in fluidized beds under realistic calcination
1669 conditions. *J. Environ. Eng.-ASCE* **2009**, 135, 404-410.
- 1670 89. Valverde, J. M.; Sanchez-Jimenez, P. E.; Perez-Maqueda, L. A. Calcium-looping for post-
1671 combustion CO₂ capture. On the adverse effect of sorbent regeneration under CO₂.
1672 *Applied Energy* **2014**, 126, 161-171.
- 1673 90. Valverde, J. M.; Sanchez-Jimenez, P. E.; Perez-Maqueda, L. A. Effect of Heat
1674 Pretreatment/Recarbonation in the Ca-Looping Process at Realistic Calcination
1675 Conditions. *Energy & Fuels* **2014**, 28, 4062-4067.

- 1676 91. Valverde, J. M.; Sanchez-Jimenez, P. E.; Perez-Maqueda, L. A. Ca-looping for
1677 postcombustion CO₂ capture: A comparative analysis on the performances of dolomite
1678 and limestone. *Applied Energy* **2015**, 138, 202-215.
- 1679 92. Grasa, G. S.; Abanades, J. C. CO₂ capture capacity of CaO in long series of
1680 carbonation/calcination cycles. *Industrial & Engineering Chemistry Research* **2006**, 45,
1681 8846-8851.
- 1682 93. Alvarez, D.; Abanades, J. C. Determination of the critical product layer thickness in the
1683 reaction of CaO with CO₂. *Industrial & Engineering Chemistry Research* **2005**, 44, 5608-
1684 5615.
- 1685 94. Alvarez, D.; Abanades, J. C. Pore-size and shape effects on the recarbonation
1686 performance of calcium oxide submitted to repeated calcination/recarbonation cycles.
1687 *Energy & Fuels* **2005**, 19, 270-278.
- 1688 95. Salvador, C.; Lu, D.; Anthony, E. J.; Abanades, J. C. Enhancement of CaO for CO₂
1689 capture in an FBC environment. *Chemical Engineering Journal* **2003**, 96, 187-195.
- 1690 96. Grasa, G.; Murillo, R.; Alonso, M.; Abanades, J. C. Capture of CO₂ from combustion
1691 gases in a fluidized bed of CaO. *AIChE J.* **2009**, 55, 1246-1255.
- 1692 97. Perez-Maqueda, L. A.; Criado, J. M.; Real, C. Kinetics of the initial stage of sintering
1693 from shrinkage data: Simultaneous determination of activation energy and kinetic
1694 model from a single nonisothermal experiment. *J. Am. Ceram. Soc.* **2002**, 85, 763-768.
- 1695 98. Valverde, J. M.; Sanchez-Jimenez, P. E.; Perejon, A.; Perez-Maqueda, L. A. Role of
1696 Looping-Calcination Conditions on Self-Reactivation of Thermally Pretreated CO₂
1697 Sorbents Based on CaO. *Energy & Fuels* **2013**, 27, 3373-3384.
- 1698 99. Borgwardt, R. H. Sintering of nascent calcium-oxide. *Chemical Engineering Science*
1699 **1989**, 44, 53-60.
- 1700 100. Valverde, J. M.; Sanchez-Jimenez, P. E.; Perejon, A.; Perez-Maqueda, L. A. Constant
1701 rate thermal analysis for enhancing the long-term CO₂ capture of CaO at Ca-looping
1702 conditions. *Applied Energy* **2013**, 108, 108-120.
- 1703 101. Valverde, J. M.; Sanchez-Jimenez, P. E.; Perejon, A.; Perez-Maqueda, L. A. CO₂
1704 multicyclic capture of pretreated/doped CaO in the Ca-looping process. Theory and
1705 experiments. *Physical Chemistry Chemical Physics* **2013**, 15, 11775-11793.
- 1706 102. Wang, J.; Manovic, V.; Wu, Y.; Anthony, E. J. A study on the activity of CaO-based
1707 sorbents for capturing CO₂ in clean energy processes. *Applied Energy* **2010**, 87, 1453-
1708 1458.
- 1709 103. Manovic, V.; Charland, J. P.; Blamey, J.; Fennell, P. S.; Lu, D. Y.; Anthony, E. J. Influence
1710 of calcination conditions on carrying capacity of CaO-based sorbent in CO₂ looping
1711 cycles. *Fuel* **2009**, 88, 1893-1900.
- 1712 104. Allen, J. P.; Marmier, A.; Parker, S. C. Atomistic Simulation of Surface Selectivity on
1713 Carbonate Formation at Calcium and Magnesium Oxide Surfaces. *J. Phys. Chem. C*
1714 **2012**, 116, 13240-13251.
- 1715 105. Besson, R.; Favregeon, L. Atomic-Scale Study of Calcite Nucleation in Calcium Oxide. *J.*
1716 *Phys. Chem. C* **2013**, 117, 8813-8821.
- 1717 106. Besson, R.; Vargas, M. R.; Favregeon, L. CO₂ adsorption on calcium oxide: An atomic-
1718 scale simulation study. *Surf. Sci.* **2012**, 606, 490-495.
- 1719 107. Hyatt, E. P.; Cutler, I. B.; Wadsworth, M. E. Calcium Carbonate Decomposition in
1720 Carbon Dioxide Atmosphere. *J. Am. Ceram. Soc.* **1958**, 41, 70-74.
- 1721 108. Valverde, J. M.; Sanchez-Jimenez, P. E.; Perez-Maqueda, L. A. Limestone calcination
1722 nearby equilibrium: kinetics, CaO crystal structure, sintering and reactivity. *J. Phys.*
1723 *Chem. C* **2015**, 119, 1623-1641.
- 1724 109. Borgwardt, R. H. Calcium oxide sintering in atmospheres containing water and carbon
1725 dioxide. *Industrial & Engineering Chemistry Research* **1989**, 28, 493-500.

- 1726 110. Stanmore, B. R.; Gilot, P. Review—calcination and carbonation of limestone during
1727 thermal cycling for CO₂ sequestration. *Fuel Processing Technology* **2005**, 86, 1707-
1728 1743.
- 1729 111. Grasa, G.; Murillo, R.; Alonso, M.; Abanades, J. C. Application of the random pore
1730 model to the carbonation cyclic reaction. *AIChE Journal* **2009**, 55, 1246-1255.
- 1731 112. Bhatia, S. K.; Perlmutter, D. D. Effect of the product layer on the kinetics of the CO₂-
1732 lime reaction. *AIChE Journal* **1983**, 29, 79-86.
- 1733 113. Sun, Z.; Luo, S.; Qi, P.; Fan, L.-S. Ionic diffusion through Calcite (CaCO₃) layer during the
1734 reaction of CaO and CO₂. *Chemical Engineering Science* **2012**, 81, 164-168.
- 1735 114. Li, Z.; Sun, H.; Cai, N. Rate equation theory for the carbonation reaction of CaO with
1736 CO₂. *Energy & Fuels* **2012**, 26, 4607-4616.
- 1737 115. Li, Z.-s.; Fang, F.; Tang, X.-y.; Cai, N.-s. Effect of temperature on the carbonation
1738 reaction of CaO with CO₂. *Energy & Fuels* **2012**, 26, 2473-2482.
- 1739 116. Kierzkowska, A. M.; Pacciani, R.; Müller, C. R. CaO-Based CO₂ sorbents: from
1740 fundamentals to the development of new, highly effective materials. *ChemSusChem*
1741 **2013**, 6, 1130-1148.
- 1742 117. Chrissafis, K.; Dagounaki, C.; Paraskevopoulos, K. M. The effects of procedural variables
1743 on the maximum capture efficiency of CO₂ using a carbonation/calcination cycle of
1744 carbonate rocks. *Thermochimica Acta* **2005**, 428, 193-198.
- 1745 118. Readman, J. E.; Blom, R. The use of in situ powder X-ray diffraction in the investigation
1746 of dolomite as a potential reversible high-temperature CO₂ sorbent. *Physical Chemistry
1747 Chemical Physics* **2005**, 7, 1214-1219.
- 1748 119. Beruto, D. T.; Vecchiattini, R.; Giordani, M. Effect of mixtures of H₂O (g) and CO₂ (g) on
1749 the thermal half decomposition of dolomite natural stone in high CO₂ pressure regime.
1750 *Thermochimica Acta* **2003**, 404, 25-33.
- 1751 120. Galai, H.; Pijolat, M.; Nahdi, K.; Trabelsi-Ayadi, M. Mechanism of growth of MgO and
1752 CaCO₃ during a dolomite partial decomposition. *Solid State Ionics* **2007**, 178, 1039-
1753 1047.
- 1754 121. Rodriguez-Navarro, C.; Kudlacz, K.; Ruiz-Agudo, E. The mechanism of thermal
1755 decomposition of dolomite: New insights from 2D-XRD and TEM analyses. *American
1756 Mineralogist* **2012**, 97, 38-51.
- 1757 122. Silaban, A.; Narcida, M.; Harrison, D. P. Characteristics of the reversible reaction
1758 between CO₂(g) and calcined dolomite. *Chemical Engineering Communications* **1996**,
1759 146, 149-162.
- 1760 123. Albrecht, K. O.; Wagenbach, K. S.; Satrio, J. A.; Shanks, B. H.; Wheelock, T. D.
1761 Development of a CaO-Based CO₂ sorbent with improved cyclic stability. *Industrial &
1762 Engineering Chemistry Research* **2008**, 47, 7841-7848.
- 1763 124. Sultan, D. S.; Müller, C. R.; Dennis, J. S. Capture of CO₂ using sorbents of calcium
1764 magnesium acetate (CMA). *Energy & Fuels* **2010**, 24, 3687-3697.
- 1765 125. Yang, X.; Zhao, L.; Yang, S.; Xiao, Y. Investigation of natural CaO-MgO sorbent for CO₂
1766 capture. *Asia-Pacific Journal of Chemical Engineering* **2013**, 8, 906-915.
- 1767 126. Coppola, A.; Scala, F.; Salatino, P.; Montagnaro, F. Fluidized bed calcium looping cycles
1768 for CO₂ capture under oxy-firing calcination conditions: Part 2. Assessment of dolomite
1769 vs. limestone. *Chemical Engineering Journal* **2013**, 231, 544-549.
- 1770 127. Valverde, J. M.; Sanchez-Jimenez, P. E.; Perez-Maqueda, L. A.; Quintanilla, M. A. S.;
1771 Perez-Vaquero, J. Role of crystal structure on CO₂ capture by limestone derived CaO
1772 subjected to carbonation/recarbonation/calcination cycles at Ca-looping conditions.
1773 *Applied Energy* **2014**, 125, 264-275.
- 1774 128. Sanchez-Jimenez, P. E.; Valverde, J. M.; Perez-Maqueda, L. A. Multicyclic conversion of
1775 limestone at Ca-looping conditions: The role of solid-state diffusion controlled
1776 carbonation. *Fuel* **2014**, 127, 131-140.

- 1777 129. Valverde, J. M.; Sanchez-Jimenez, P. E.; Perez-Maqueda, L. A. Relevant influence of
1778 limestone crystallinity on CO₂ capture in the Ca-Looping technology at realistic
1779 calcination conditions. *Environmental Science & Technology* **2014**, 48, 9882-9889.
- 1780 130. Beruto, D.; Barco, L.; Searcy, A. W. CO₂-catalyzed surface-area and porosity changes in
1781 high-surface-area cao aggregates. *J. Am. Ceram. Soc.* **1984**, 67, 512-515.
- 1782 131. Wang, Y.; Thomson, W. J. The effects of steam and carbon dioxide on calcite
1783 decomposition using dynamic X-ray diffraction. *Chemical Engineering Science* **1995**, 50,
1784 1373-1382.
- 1785 132. Khinast, J.; Krammer, G. F.; Brunner, C.; Staudinger, G. Decomposition of limestone:
1786 The influence of CO₂ and particle size on the reaction rate. *Chemical Engineering*
1787 *Science* **1996**, 51, 623-634.
- 1788 133. Beruto, D. T.; Searcy, A. W.; Kim, M. G. Microstructure, kinetic, structure,
1789 thermodynamic analysis for calcite decomposition: free-surface and powder bed
1790 experiments. *Thermochimica Acta* **2004**, 424, 99-109.
- 1791 134. Haul, R. A. W.; Heystek, H. Differential thermal analysis of the dolomite
1792 decomposition. *Am. Miner.* **1952**, 37, 166-179.
- 1793 135. Caceres, P. G.; Attiogbe, E. K. Thermal decomposition of dolomite and the extraction of
1794 its constituents. *Minerals Engineering* **1997**, 10, 1165-1176.
- 1795 136. Samtani, M.; Skrzypczak-Jankun, E.; Dollimore, D.; Alexander, K. Thermal analysis of
1796 ground dolomite, confirmation of results using an X-ray powder diffraction
1797 methodology. *Thermochimica Acta* **2001**, 367-368, 297-309.
- 1798 137. Arai, Y., *Chemistry of Power Production*, Chapman & Hall, Glasgow, 1996.
- 1799 138. Manovic, V.; Anthony, E. J. Thermal activation of CaO-based sorbent and self-
1800 reactivation during CO₂ capture looping cycles. *Environmental Science & Technology*
1801 **2008**, 42, 4170-4174.
- 1802 139. Manovic, V.; Anthony, E. J.; Loncarevic, D. Looping cycles with CaO-based sorbent
1803 pretreated in at high temperature. *Chemical Engineering Science* **2009**, 64, 3236-3245.
- 1804 140. Ozcan, D. C.; Shanks, B. H.; Wheelock, T. D. Improving the stability of a CaO-based
1805 sorbent for CO₂ by thermal pretreatment. *Industrial & Engineering Chemistry Research*
1806 **2011**, 50, 6933-6942.
- 1807 141. Alonso, M.; Lorenzo, M.; Gonzalez, B.; Abanades, J. C. Precalcination of CaCO₃ as a
1808 method to stabilize cao performance for CO₂ capture from combustion gases. *Energy &*
1809 *Fuels* **2011**, 25, 5521-5527.
- 1810 142. Baláz, P., *Mechanochemistry in nanoscience and minerals engineering*, Springer, Berlin,
1811 2008.
- 1812 143. Heitjans, P.; Indris, S. Fast diffusion in nanocrystalline ceramics prepared by ball
1813 milling. *Journal of Materials Science* **2004**, 39, 5091-5096.
- 1814 144. Perejon, A.; Murafa, N.; Sanchez-Jimenez, P. E.; Criado, J. M.; Subrt, J.; Dianez, M. J.;
1815 Perez-Maqueda, L. A. Direct mechanosynthesis of pure BiFeO₃ perovskite
1816 nanoparticles: reaction mechanism. *Journal of Materials Chemistry C* **2013**, 1, 3551-
1817 3562.
- 1818 145. Suryanarayana, C. Mechanical alloying and milling. *Progress in Materials Science* **2001**,
1819 46, 1-184.
- 1820 146. Kong, L. B.; Zhang, T. S.; Ma, J.; Boey, F. Progress in synthesis of ferroelectric ceramic
1821 materials via high-energy mechanochemical technique. *Progress in Materials Science*
1822 **2008**, 53, 207-322.
- 1823 147. Perejon, A.; Sanchez-Jimenez, P. E.; Perez-Maqueda, L. A.; Criado, J. M.; de Paz, J. R.;
1824 Saez-Puche, R.; Maso, N.; West, A. R. Single phase, electrically insulating, multiferroic
1825 La-substituted BiFeO₃ prepared by mechanosynthesis. *Journal of Materials Chemistry C*
1826 **2014**, 2, 8398-8411.
- 1827 148. Kronenberg, A.; Yund, R.; Giletti, B. Carbon and oxygen diffusion in calcite: Effects of
1828 Mn content and P H₂O. *Phys Chem Minerals* **1984**, 11, 101-112.

- 1829 149. Anderson, T. F. Self-diffusion of carbon and oxygen in calcite by isotope exchange with
1830 carbon dioxide. *Journal of Geophysical Research* **1969**, 74, 3918-3932.
- 1831 150. Akgornpeak, A.; Witoon, T.; Mungcharoen, T.; Limtrakul, J. Development of synthetic
1832 CaO sorbents via CTAB-assisted sol-gel method for CO₂ capture at high temperature.
1833 *Chemical Engineering Journal* **2014**, 237, 189-198.
- 1834 151. Pacciani, R.; Muller, C. R.; Davidson, J. F.; Dennis, J. S.; Hayhurst, A. N. Performance of
1835 a Novel Synthetic Ca-Based Solid Sorbent Suitable for Desulfurizing Flue Gases in a
1836 Fluidized Bed. *Industrial & Engineering Chemistry Research* **2009**, 48, 7016-7024.
- 1837 152. Strohle, J.; Junk, M.; Kremer, J.; Galloy, A.; Epple, B. Carbonate looping experiments in
1838 a 1 MWth pilot plant and model validation. *Fuel* **2014**, 127, 13-22.
- 1839 153. Chang, M. H.; Huang, C. M.; Liu, W. H.; Chen, W. C.; Cheng, J. Y.; Chen, W.; Wen, T. W.;
1840 Ouyang, S.; Shen, C. H.; Hsu, H. W. Design and Experimental Investigation of the
1841 Calcium Looping Process for 3-kW(th) and 1.9-MWth Facilities. *Chem. Eng. Technol.*
1842 **2013**, 36, 1525-1532.
- 1843 154. Alonso, M.; Diego, M. E.; Perez, C.; Chamberlain, J. R.; Abanades, J. C. Biomass
1844 combustion with in situ CO₂ capture by CaO in a 300 kWth circulating fluidized bed
1845 facility. *International Journal of Greenhouse Gas Control* **2014**, 29, 142-152.
- 1846 155. Hanak, D. P.; Anthony, E. J.; Manovic, V. A review of developments in pilot-plant
1847 testing and modelling of calcium looping process for CO₂ capture from power
1848 generation systems. *Energy & Environmental Science* **2015**, 8, 2199-2249.
- 1849